

GENE THERAPY

Slowing late infantile Batten disease by direct brain parenchymal administration of a rh.10 adeno-associated virus expressing *CLN2*

Dolan Sondhi¹, Stephen M. Kaminsky¹, Neil R. Hackett¹, Odelya E. Pagovich¹, Jonathan B. Rosenberg¹, Bishnu P. De¹, Alvin Chen¹, Benjamin Van de Graaf¹, Jason G. Mezey^{1,2}, Grace W. Mammen¹, Denesy Mancenido¹, Fang Xu¹, Barry Kosofsky³, Kaleb Yohay^{3*}, Stefan Worgall^{1,3}, Robert J. Kaner^{1,4}, Mark Souwedaine⁵, Bruce M. Greenwald³, Michael Kaplitt⁵, Jonathan P. Dyke⁶, Douglas J. Ballon^{1,6}, Linda A. Heier⁶, Szilard Kiss⁷, Ronald G. Crystal^{1,4†}

Copyright © 2020
The Authors, some
rights reserved;
exclusive licensee
American Association
for the Advancement
of Science. No claim
to original U.S.
Government Works

Late infantile Batten disease (CLN2 disease) is an autosomal recessive, neurodegenerative lysosomal storage disease caused by mutations in the *CLN2* gene encoding tripeptidyl peptidase 1 (TPP1). We tested intraparenchymal delivery of AAVrh.10hCLN2, a nonhuman serotype rh.10 adeno-associated virus vector encoding human *CLN2*, in a nonrandomized trial consisting of two arms assessed over 18 months: AAVrh.10hCLN2-treated cohort of 8 children with mild to moderate disease and an untreated, Weill Cornell natural history cohort consisting of 12 children. The treated cohort was also compared to an untreated European natural history cohort of CLN2 disease. The vector was administered through six burr holes directly to 12 sites in the brain without immunosuppression. In an additional safety assessment under a separate protocol, five children with severe CLN2 disease were treated with AAVrh.10hCLN2. The therapy was associated with a variety of expected adverse events, none causing long-term disability. Induction of systemic anti-AAVrh.10 immunity was mild. After therapy, the treated cohort had a 1.3- to 2.6-fold increase in cerebral spinal fluid TPP1. There was a slower loss of gray matter volume in four of seven children by MRI and a 42.4 and 47.5% reduction in the rate of decline of motor and language function, compared to Weill Cornell natural history cohort ($P < 0.04$) and European natural history cohort ($P < 0.0001$), respectively. Intraparenchymal brain administration of AAVrh.10hCLN2 slowed the progression of disease in children with CLN2 disease. However, improvements in vector design and delivery strategies will be necessary to halt disease progression using gene therapy.

INTRODUCTION

CLN2 disease [also referred to as late infantile neuronal ceroid lipofuscinosis (LINCL), late infantile Batten disease, Janky-Bielschowsky disease, and tripeptidyl peptidase 1 (TPP1) deficiency] is a uniformly fatal childhood autosomal recessive neurodegenerative lysosomal storage disorder caused by mutations in the *CLN2* gene (1–6). The disease affects the central nervous system (CNS) and retina, with typical onset between ages 2 and 4 years old. The clinical course is characterized by progressive neurologic decline with cognitive impairment, visual failure, seizures, deterioration of motor and language skills, and death by ages 10 to 12 (2, 5, 7, 8). The disease is caused by mutations in the *CLN2* gene, which encodes lysosomal TPP1, an enzyme that cleaves tripeptides from the N terminus of polypeptides imported into the lysosome (1, 9). The loss of TPP1 activity leads to accumulation of storage material in lysosomes, characterized as autofluorescent intracellular deposits by light microscopy (2, 10). There is allelic heterogeneity, but two *CLN2* variants,

G3556C (c.509-1G>C; intron 7 splice defect) and C3670T (c.622C>T; nonsense Arg²⁰⁸ to stop), are responsible for most cases in Caucasian populations (www.ucl.ac.uk/ncl/CLN2mutationtable.htm) (1, 10, 11).

CLN2 disease has several features making it a good target for gene therapy using an adeno-associated virus (AAV) vector expressing the normal human *CLN2* coding sequence (12–19). AAV vectors are efficient in transferring genes to the CNS, mediating persistent expression (20–25). Genotype/phenotype comparisons suggest that the severe phenotype should be ameliorated with an increase of CNS TPP1 amount to 5 to 10% of normal (12, 26). TPP1 is a secreted protein capable of cross-correcting neighboring cells via uptake by the mannose-6-phosphate receptor (27–29). Therefore, it is not necessary to transfer the normal *CLN2* complementary DNA (cDNA) to all of the cells in the CNS, because the corrected cells will secrete TPP1 protein, which will be taken up to correct neighboring cells. The concept that delivery of TPP1 to the CNS can be effective in treating CLN2 CNS disease is supported by the success of cerliponase alfa, a recombinant human TPP1 protein therapy administered biweekly to cerebral spinal fluid (CSF) via a CNS reservoir, in slowing the progression of the CNS disease (30–32). If AAV-mediated CNS gene therapy with the *CLN2* coding sequence could provide sufficient amounts of TPP1 throughout the CNS, it could provide a one-time therapy to treat the disease.

On the basis of efficacy studies in *CLN2*^{-/-} mice and CNS biodistribution and safety studies in nonhuman primates (33–35), we chose the AAV serotype rh.10 expressing the normal human *CLN2* coding sequence (AAVrh.10hCLN2) to treat children with CLN2

¹Department of Genetic Medicine, Weill Cornell Medical College, New York, NY 10065, USA. ²Department of Biological Statistics and Computational Biology, Cornell University, Ithaca, NY 14853, USA. ³Department of Pediatrics, Weill Cornell Medical College, New York, NY 10065, USA. ⁴Department of Medicine, Weill Cornell Medical College, New York, NY 10065, USA. ⁵Department of Neurological Surgery, Weill Cornell Medical College, New York, NY 10065, USA. ⁶Department of Radiology, Weill Cornell Medical College, New York, NY 10065, USA. ⁷Department of Ophthalmology, Retina Service, Weill Cornell Medical College, New York, NY 10065, USA. *Present address: Departments of Pediatrics and Neurology, NYU Langone Health, New York, NY 10016, USA.

†Corresponding author. Email: geneticmedicine@med.cornell.edu

disease. The hypothesis of the study was that direct CNS administration of AAVrh.10hCLN2 was safe and would slow down the progression of the neurologic disease.

RESULTS

We tested intraparenchymal delivery of AAVrh.10hCLN2, a non-human serotype rh.10 AAV vector coding for human CLN2 (fig. S1). The vector, AAVrh.10hCLN2 [total dose of 2.85×10^{11} to 9.0×10^{11} genome copies (gc)], was delivered directly via catheter into the CNS via six burr holes (three bilaterally), with equal doses to two sites per burr hole (2.4×10^{10} to 7.5×10^{10} gc in 150 μ l per site) (fig. S2). The study was designed as a nonrandomized trial comparing a treatment group that received AAVrh.10hCLN2 (cohort 1; $n = 8$) and a non-treated natural history control cohort (“Weill Cornell natural history control cohort,” cohort 2; $n = 12$). The study population was limited to children with CLN2 disease with specific genotypes and severity criteria, limiting the inclusion to those with mild to moderate disease as assessed by a clinical neurologic rating scale (table S1) (4, 36).

As the trial progressed, we participated in a collaborative publication of the natural history of untreated CLN2 disease, comparing disease progression of the Weill Cornell natural history control cohort to that of the “European DEM Child Natural History” cohort (5). Because the DEM Child cohort is the untreated cohort from which natural history controls were used for the regulatory approval of cerliponase alfa therapy, although not part of our original design, we have used the European DEM Child Natural History cohort data as a replication control cohort ($n = 41$, “DEM Child Natural History Replication Cohort,” cohort 3).

Last, there were five children who had severe disease and did not meet the “mild to moderate” entry criteria (Weill Cornell LINCL scale <6) (4) and/or did not fit the genotype entry criteria. Under a separate protocol, these five children were treated and assessed for additional safety data (“therapy/safety-only cohort,” cohort 4).

Description of the primary treatment and control cohorts

Cohort 1 (the therapy cohort, $n = 8$, V1 to V8) included four females and four males (Table 1). Of the eight subjects, three subjects

were homozygous for either g.C3670T or g.G3556C, and two were compound heterozygous for both genotypes. The remaining three were heterozygous for either g.C3670T or g.G3556C and a different mutation. The average age of first reported symptoms was 29 months (range, 16 to 48 months). In seven of eight subjects in this group, the first reported symptom was speech delay, accompanied in some subjects by motor, balance, cognition, and behavioral abnormalities. Six of the eight had the age of first seizure between 30 and 50 months of age and two between 18 and 25 months. As described above, subject V8 was not included in the analysis.

Cohort 2 (the Weill Cornell natural history cohort, $n = 12$, C1 to C12) included eight females and four males (Table 1). Ninety-two percent (11 of 12) were homozygous or heterozygous for either g.C3670T or g.G3556C, with 5 (42%) heterozygous for g.C3670T and g.G3556C and 2 (17%) homozygous for g.C3670T. The remaining four were heterozygous for either g.C3670T or g.G3556C and a different mutation (see Table 2 for genotypes). Fifty-five percent manifested symptoms at about 24 months, and 45% had symptoms by 36 months. In 10 of 12, the first reported symptom was speech delay, accompanied in some by balance, motor, cognition, and behavioral issues. Almost all had the age of first seizure between 30 and 50 months of age, with the latest at 54 months.

Description of the ancillary cohorts

The European DEM Child Natural History Replication Control Cohort (cohort 3) consisted of 41 CLN2 genotype-confirmed subjects (Table 1) (5). Twenty-four were males, and 17 were females. The mutations included 71% heterozygous or homozygous for g.C3670T or g.G3556C. Of those, 42% were homozygous at both alleles for g.C3670T, and 7% were homozygous for g.G3556C. Of the remainder, 39% were either heterozygous for both mutations or heterozygous with a different mutation; 12% did not have either of the two common mutations. The average age of first observed clinical symptom was 33 months (range, 12 to 53 months). For the majority (88%), the age of first seizure was 30 to 50 months, two had the first seizure at 0 to 30 months, two at 50 to 70 months and one at 106 months.

The safety-only-treated cohort (cohort 4) was composed of 5 children ($n = 4$ females and $n = 1$ male, S1 to S5; Table 1). The

Table 1. Study cohorts. M, male; F, female; DEM Child, a consortium that studies the natural history of neuronal ceroid lipofuscinoses disorders.

Group	Number of subjects	Sex	Age at report of the first symptom (months)	Age of first reported seizure (months)	Most common first symptom
Cohort 1: treatment*	8, 7 with follow-up	4 M/4 F	16–48	18–50	Speech delay
Cohort 2: no treatment control†	12	4 M/8 F	24–36	30–54	Speech delay
Cohort 3: DEM Child Replication Control‡	41	24 M/17 F	12–53	0–106	Seizures
Cohort 4: treatment/safety only§	5	1 M/4 F	24–42	30–36	Speech delay

*Mild to moderate disease; of the $n = 8$, seven had follow-up during the 18-month study period. †The pretherapy data from subject S5 (cohort 4) over the 5 months before therapy was used as part of the Weill Cornell natural history data (referred to as subject C3 in cohort 2). Before receiving treatment, subject C3 had two assessments that were 5 months apart. ‡Cohort 3: The untreated European DEM Child Cohort was used as a replication control group (5). §Cohort 4: treated children with severe disease, used for additional safety data.

Table 2. Assessment of cohort 1 with the motor + language parameters. The motor and language data are provided for all subjects in cohort 1. The rows highlighted in light gray are before administration, dark gray is vector administration, and the unshaded rows are post-administration visits. The clinical assessment of motor + language was performed prospectively using defined standard operating procedures (SOPs) based on three to four observers, with specific rules on how the data were evaluated. The primary, on-site assessor was a pediatric neurologist who had been trained on implementing the scale. The assessment of each child was videotaped by a trained technician after an SOP for recording the assessment and editing for review by two to three other pediatric neurologists who were trained on implementing the scale. All were blinded to the subjects' treatment status. In the event of discrepancy of more than one point between the two blinded scorers, a third pediatric neurologist, also blinded, scored the video to act as a tie-breaker. The final score was an average of the assessment of three to four reviewers (primary two to three additional reviewers), minimizing bias and subjective interpretation. The data provided here are the final score.

Subject*/genotype	Study visit†	Age at assessment (months)	Time before or after vector administration (months)	Motor score‡	Language score§	Total score
V1¶	1	83.0	-4.6	1.0	1.7	2.7
G3556C/G3556C	2	87.4	-0.2	1.3	2.0	3.3
	Vector	87.6	0	-	-	-
		88.8	+1.2	1.0	1.0	2.0
	4	93.9	+6.3	1.0	1.3	2.3
	5	99.9	+12.3	1.0	1.0	2.0
	6	106.6	+19.0	0.0	1.0	1.0
V2#	1	39.6	-2.5	2.7	2.0	4.7
C3670T/G3556C	2	41.0	-1.1	3.0	2.0	5.0
	3	42.0	-0.1	2.7	2.0	4.7
	Vector	42.1	0	-	-	-
	4	43.1	+1.0	3.0	2.0	5.0
	5	48.4	+6.3	3.0	2.0	5.0
	6	54.6	+12.5	2.3	2.0	4.3
	7	60.1	+18.0	2.3	2.0	4.3
V3**	1	52.2	-1.5	1.0	1.0	2.0
G3556C/G4655A	2	53.6	-0.1	1.0	1.7	2.7
	Vector	53.7	0	-	-	-
	3	54.6	+0.9	1.0	0.0	1.0
	4	60.5	+6.7	1.0	0.0	1.0
	5	65.8	+12.0	0.3	0.0	0.3
	6	72.4	+18.7	1.0	0.0	1.0
V4††	1	53.9	-2.2	2.0	1.7	3.7
G3556C/G3556C	2	55.9	-0.2	2.0	2.0	4.0
	Vector	56.1	0	-	-	-
	3	57.0	+0.9	1.3	1.0	2.3
	4	61.9	+5.8	1.0	1.0	2.0
	5	68.4	+12.3	1.0	1.3	2.3
	6	74.1	+18.0	0.0	0.0	0.0
V5‡‡	1	32.2	-1.8	2.0	1.0	3.0
G3556C/C3084T	2	33.8	-0.2	3.0	2.0	5.0
	Vector	34.0	0	-	-	-
	3	34.8	+0.8	3.0	1.7	4.7
	4	40.0	+6.0	2.0	2.0	4.0
	5	46.0	+12.0	3.0	2.0	5.0
	6	54.3	+20.3	2.0	2.0	4.0

Continued on next page

Subject*/genotype	Study visit†	Age at assessment (months)	Time before or after vector administration (months)	Motor score‡	Language score§	Total score
V6§§	1	63.1	-0.8	1.0	1.0	2.0
G3556C/G4013T	2	63.7	-0.2	1.0	1.0	2.0
	Vector	63.9	0	-	-	-
	3	65.4	+1.4	1.0	1.0	2.0
	4	69.5	+5.6	0.7	1.0	1.7
	5	95.0	+31.1	0.0	0.0	0.0
V7	1	59.5	-1.1	2.0	1.7	3.7
C3670T/G3556C	2	60.4	-0.2	2.0	1.7	3.7
	Vector	60.6	0	-	-	-
	3	61.7	+1.1	1.0	2.0	3.0
	4	67.3	+6.7	1.0	1.0	2.0
	5	73.3	+12.7	0.0	1.0	1.0
	6	77.9	+17.3	0.0	1.3	1.3
V8 ¶¶	1	57.3	-0.4	2.0	1.7	3.7
C3670T/C3670T	Vector	57.7	0	-	-	-
	2	83.9	+26.2	0.0	0.0	0.0

*Subjects V1 to V8, cohort 1, received vector administration as outlined in footnotes ¶ to ¶¶. The genotypes for each subject are provided; following are the alternate nomenclatures for each mutation: G3556C (c.509-1G>C; intron 7 splice), C3670T (c.622C>T; nonsense Arg²⁰⁸ to stop), G4665A (1094 G>A; Cys³⁶⁵Tyr), C3084T (379 C>T; Arg¹²⁷X), and G4013T (851G>T; Gly²⁴⁸Val). †Each subject typically underwent two motor + language assessments before vector administration and four assessments (scheduled for months 1, 6, 12, and 18) after administration. ‡Motor score: Scale of 0 to 3, 3 is normal, 2 is abnormal but independent, 1 is abnormal and requires assistance, and 0 is nonambulatory. §Language: Scale of 0 to 3, 3 is normal, 2 is abnormal, 1 is barely understandable and requires assistance, and 0 is unintelligible or no speech. || Composite of motor + language. ¶ Subject V1 received vector at age 87.6 months. ¶¶ Subject V2 received vector at age 42.1 months. ** Subject V3 received vector at age 53.7 months. †† Subject V4 received vector at age 56.1 months. ‡‡ Subject V5 received vector at age 34.0 months. §§ Subject V6 received vector at age 63.9 months. ||| Subject V7 received vector (lower dose, 2.85×10^{11} gc) at age 60.6 months. ¶¶¶ Subject V8 received vector (lower dose, 2.85×10^{11} gc) at age 57.7 months. V8 did not return for any of the interim follow-up visits; the study team was able to get one measurement on subject at their home location, 2.2 years after vector administration. Due to no data points in the 18- ± 1-month study period, a rate of decline was not calculated for this subject.

average age of first reported symptoms was 36 months (range, 24 to 42 months). In four of five, the first reported symptom was speech delay, accompanied in some subjects by gait, balance, motor, cognition, and behavioral issues. All had the first seizure between 30 and 36 months of age.

Safety of CNS administration of AAVrh.10hCLN2

Treatment with AAVrh.10hCLN2 was well tolerated, with minimal serious adverse events in the acute/postoperative period (0 to 14 days) and over the 18-month study period (14 days to 18 months). Vector infusion time, surgery time, and duration of anesthesia were similar for all subjects treated with CNS administration of the AAVrh.10hCLN2 vector (tables S2 and S3). Vector administration was well tolerated in both cohorts 1 and 4. The children were discharged from the hospital an average of 3.0 ± 1.0 days for cohort 1 and 5.0 ± 1.4 days for cohort 4. For analysis of safety, the data from cohorts 1 and 4 were combined. In the acute period, a severe adverse event (SAE) occurred in 6 of 13 children, including seizures, abnormal movements, and emesis (Table 3). For the seizures and abnormal movements (3 of 13), it was not possible to determine whether these were related to the administration procedure or study drug, and thus, they were ascribed to both. Other acute SAE included magnetic resonance im-

aging (MRI) identification of hematoma (1 of 13) and hemorrhagic contusion (1 of 13).

In the chronic period, there were 15 SAEs, with 3 definitely or possibly related to the study drug and 7 related to the drug administration (Table 3). Among the SAEs observed after 14 days were rare cases of increased seizures, dyskinesia, emesis, hygroma, pneumocephalus, bronchospasm, aspiration, pneumonia, and mild, transiently elevated hepatic enzymes. Elevated hepatic enzymes (ALT and AST) [alanine aminotransferase (ALT), aspartate aminotransferase (AST)] were observed in only one subject (S5, cohort 4) at month 6 and spontaneously resolved without therapy. There was no evidence of a pre-existing condition that would make this child more susceptible to liver damage from the vector. In the preclinical studies, we observed mild, intermittently elevated liver enzymes but no evidence for consistent elevated liver abnormalities (34). Assessment of CSF at 6 to 12 months in cohorts 1 and 4 showed no abnormal accumulation of inflammatory cells (table S4).

MRI assessed within 48 hours of vector administration demonstrated T2 hyperintensities (measured by T2 FLAIR), diffusion hyperintensity [measured by diffusion-weighted imaging (DWI)], and restriction of diffusion assessed by apparent diffusion coefficient (ADC) localized to the sites of vector administration (Fig. 1 and

Table 4). During the course of the study, these localized abnormalities persisted 6 to 12 months after therapy in most subjects, while in others, these abnormalities resolved (fig. S3). Quantification of the extent of the hyperintense T2 signal in the MRI data demonstrated that the average volume of the hyperintense signal represented <0.3% of the total brain volume, and there was no increase or decrease of this volume with time (table S5). There were no clinical sequelae attributable to these MRI findings. Despite the lack of clinical correlate, our working hypothesis, based on our studies in non-human primates (34), was that the MRI findings localized to the vector administration sites represented mild persistent edema/inflammation in the areas at the tip of the catheter where the highest

concentration of the vector was deposited. On the basis of this, we decided for subsequent subjects to reduce the dose by 1/2 log (from a total dose of 9×10^{11} gc divided into 12 sites) to a total dose of 2.85×10^{11} gc divided equally among 12 sites. Of the eight subjects that received the vector in cohort 1, six received the original dose, and the last two (V7 and V8) received the 1/2 log lower dose. Of the five subjects in cohort 4, three (S3, S4, and S5) received the 1/2 log lower dose. There was no association of T2 FLAIR, ADC, or DWI (Table 4), with dose for postoperative (*P* values: 1, 0.5, and 1), month 6 (*P* values: 0.2, 0.5, and 0.5), month 12 (*P* values: 1, 0.5, and 1), and month 18 (*P* values: 0.08, 0.5, and 1).

Antivector immunity after CNS administration of AAVrh.10hCLN2

Before gene transfer, only one subject (V2) had mildly detectable serum anti-AAVrh.10 neutralizing antibodies, and all others had undetectable neutralizing antibodies (Fig. 2A). In cohort 1, seven of eight subjects developed a mild increase in detectable anti-rh.10 capsid neutralizing antibodies; one subject (V2) developed higher neutralizing anti-capsid antibodies. At 18 months, the antibody responses persisted but were mostly low. In cohort 4, CNS administration of the AAVrh.10hCLN2 vector also resulted in a mild, systemic antivector humoral immune response (Fig. 2B). Four of five subjects developed a mild-systemic humoral immune response, whereas one subject (S1) developed a higher neutralizing antibody response to the AAVrh.10 capsid after CNS administration of the vector. At 18 months, the antibody response was slightly elevated for subject S2, but with a titer of <100. Statistical comparisons of antivector neutralizing antibody responses to the dose were not possible because of the small number of data points.

Table 3. Serious adverse events with direct CNS administration of AAVrh.10hCLN2 to cohorts 1 and 4. Serious adverse events (SAE), as defined by 21 Code of Federal Regulations (CFR) 312 (a).

Event	Number of events (% of total events)	
	Acute/postoperative*	Chronic†
Any serious adverse event (SAE)	6 (28.6)	15 (71.4)
Any SAE related to study drug‡	3 (14.3)	3 (14.3)
Any SAE related to drug administration‡	6 (28.6)	7 (33.3)
Specific SAE		
Episodes of increased seizures§	1 (4.8)	6 (28.6)
Dystonia	0 (0)	1 (4.8)
Episodes of increased abnormal movements	2 (9.5)	0 (0)
Emesis	1 (4.8)	1 (4.8)
Hematoma, hemorrhagic contusion	1 (4.8)	1 (4.8)
Hygroma	0 (0)	1 (4.8)
Pneumocephalus	1 (4.8)	0 (0)
Bronchospasm	0 (0)	1 (4.8)
Aspiration	0 (0)	1 (4.8)
Pneumonia	0 (0)	1 (4.8)
Elevated hepatic enzymes	0 (0)	2 (9.5)¶

*SAEs that occurred from day 0 (day of procedure/vector administration) to day 14 (14 days after vector administration); reported as number of occurrences (% all occurrences). †SAEs that occurred from month 1 (starting 15 days after the vector administration) to month 18 (540 days after vector administration); reported as number of occurrences (% all occurrences). ‡In most cases, in the actual/postoperative period, it is not possible to distinguish as to whether the SAE resulted from the study drug or the drug administration; whenever the SAE was reported as “likely” or “probably” related to the study drug, it was listed as “SAE related to study drug.” §General tonic-clonic seizures and myoclonic seizures. || Abnormal facial movements and facial twitches/dyskinesia. ¶Transient, mild elevation of ALT and AST at 6 months in S5, cohort 4, resolved without therapy; this subject received the lower dose of 2.85×10^{11} gc.

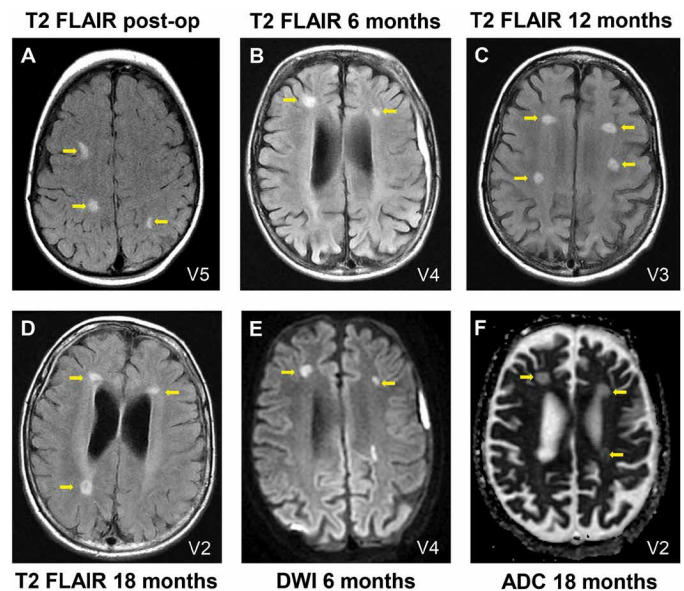


Fig. 1. Axial T2 FLAIR, DWI, and ADC MRI assessment of participants after therapy. MRI abnormalities were localized at the sites of the catheter tips, where there is the highest concentration of the administered vector. (A to D) Examples of T2 FLAIR. (A) Participant V5, 1 day after administration; (B) V4, 6 months; (C) V3, 12 months; (D) V2, 18 months. (E) Example of DWI, participant V4, 6 months. (F) Example of ADC, participant V2, 18 months. Yellow arrows identify the abnormalities. See Table 4 for the complete dataset of T2 FLAIR, DWI, and ADC abnormalities observed.

Table 4. MRI T2 hyperintensity, DWI restriction, and/or ADC at sites of administration. "T2," T2 hyperintensities localized to the site of vector administration as assessed by T2 FLAIR; "DWI," hyperintensities localized to the site of vector administration as assessed via DWI; "ADC," apparent diffusion coefficient, DWI data quantified. "-" indicates the absence of T2 hyperintensities, and "+" indicates the presence of T2 hyperintensities. "-/-" indicates the absence of DWI hyperintensities and of the associated diffusion restriction, "+/-" indicates the presence of DWI hyperintensities but the absence of the associated diffusion restriction, "+/+ " indicates the presence of DWI hyperintensities and also of the associated diffusion restriction, and * ND, not done.

Cohort	Subject	Total dose (gc)	Before transfer		Postoperative		Month 6		Month 12		Month 18	
			T2	DWI/ADC	T2	DWI/ADC	T2	DWI/ADC	T2	DWI/ADC	T2	DWI/ADC
1	V1	9.0×10^{11}	-	-/-	+	+/+	+	+/+	+	+/-	+	-/-
	V2	9.0×10^{11}	-	-/-	+	-/-	+	+/+	+	+/+	+	+/+
	V3	9.0×10^{11}	-	-/-	+	+/+	+	-/-	+	-/-	+	-/-
	V4	9.0×10^{11}	-	-/-	+	-/-	+	+/+	+	+/+	+	-/-
	V5	9.0×10^{11}	-	-/-	+	-/-	+	-/-	+	+/-	+	+/-
	V6	9.0×10^{11}	-	-/-	+	+/+	-	-/-	ND*	ND	ND	ND
	V7	2.85×10^{11}	-	-/-	+	+/+	+	-/-	ND	ND	ND	ND
	V8	2.85×10^{11}	-	-/-	+	+/+	ND	ND	ND	ND	-†	-/-†
4	S1‡	9.0×10^{11}	-	-/-	+	+/+	ND	ND	ND	ND	ND	ND
	S2	9.0×10^{11}	-	-/-	+	+/+	+	-/-	-	-/-	+	-/-
	S3	2.85×10^{11}	-	-/-	+	+/+	-	-/-	+	+/-	-	-/-
	S4	2.85×10^{11}	-	-/-	+	+/+	-	-/-	+	-/-	+	-/-
	S5	2.85×10^{11}	-	-/-	+	+/+	-†	-/-†	-†	-/-†	ND	ND

Some of the follow-up MRIs were not done because of the difficulty of travel to Weill Cornell for the MRI; under these circumstances, whenever possible, the study team did the clinical assessment of the child at the subject's home. †For subjects V8 and S5, some of the MRI scans were at their local hospitals. ‡Subject S1 discontinued from further participation in the study, and no follow-up MRI data were available thereafter.

For cohort 1, anti-AAVrh.10 neutralizing antibodies were also assessed in the CSF for whom pre- and posttreatment CSF samples were available ($n = 5$). No detectable anti-rh.10 capsid neutralizing antibodies were observed (Fig. 2C).

Blood T cell responses to the AAVrh.10 capsid and the CLN2 transgene were assessed by interferon- γ ELISpot (enzyme-linked immune absorbent spot). Blood mononuclear cells obtained from the subjects before therapy at screening and before vector administration and at days 7 and 14 and months 1, 6, 12, and 18 after vector administration were stimulated with AAVrh.10 capsid and CLN2 transgene peptide library pools. There were sporadic, but not persistent, mild responses among the samples to the vector capsid or transgene, with no correlation to time after vector administration (fig. S4, A and B). Subjects S2 and S4 had mildly elevated ELISpots. This could be a function of the CLN2 genotype because these two subjects each have one allele that is unique among study participants. Qualitatively, there was neither correlation of neutralizing antibodies titers and the minor, specific T cell responses nor with vector dose.

Assessment of treatment efficacy

Follow-up data over the 18-month study period were available for analysis from seven of the eight treated children in cohort 1. The parameters used to assess efficacy included (i) TPP1 amount in CSF, (ii) assessment of MRI percent gray matter volume, (iii) vision parameters, and (iv) neurologic clinical assessment of motor + language scale. All three CNS parameters suggested a positive treatment effect (Figs. 3 to 5 and figs. S5 and S6). The limited amount of vision-related data showed no treatment effect. The ITQoL-PF97 or CHQ-PF50 quality of life questionnaires and Mullen scales were

used before and after therapy to question the parents and assess the children, respectively. We found these scales to be highly variable, with no measurable differences between cohort 1 and the control cohort 2 (figs. S7 and S8 and table S6).

All AAVrh.10hCLN2-treated patients for whom pre- and post-treatment CSF samples were available ($n = 5$) had increased TPP1 in the CSF compared to the pretreatment values (Fig. 3A). Quantification of CSF TPP1 6 to 12 months after therapy demonstrated a 1.3- to 2.6-fold increase over pretherapy values. When compared to TPP1 in normals, the pretreatment values ranged from 5 to 13 percent of normal, and the posttreatment values ranged from 8 to 26% ($P < 0.03$; Fig. 3B).

Untreated children with CLN2 disease have a decrease in % gray matter volume from ages 2 to 6 (36, 37). The percent gray matter volume over time of the treated children in cohort 1 was compared to the untreated children with CLN2 disease (Fig. 4 and figs. S4 and S5). Two of the seven treated children had only a single scan after treatment, insufficient to calculate the standard error of the rate of decline of percent gray matter. For the five children with two or more posttherapy scans, three had rates of decline in percent gray matter volume less than the untreated CLN2 children. Of the two children with only one posttherapy scan, one of two had percent gray matter decline slower than that of the untreated children. Two children, the youngest in the cohort, who may not yet have been of age for rapid change in gray matter to occur were likely to have indistinguishable effects.

The ocular and CNS disorders associated with CLN2 disease are distinct and develop independently. The ocular findings are typified by a gradually progressive retinal degeneration, commencing at the outer retina (specifically in the retinal pigmented epithelium and photoreceptors in a bull's eye pattern), and progressing from the central macula to the peripheral retina, symmetrically between the

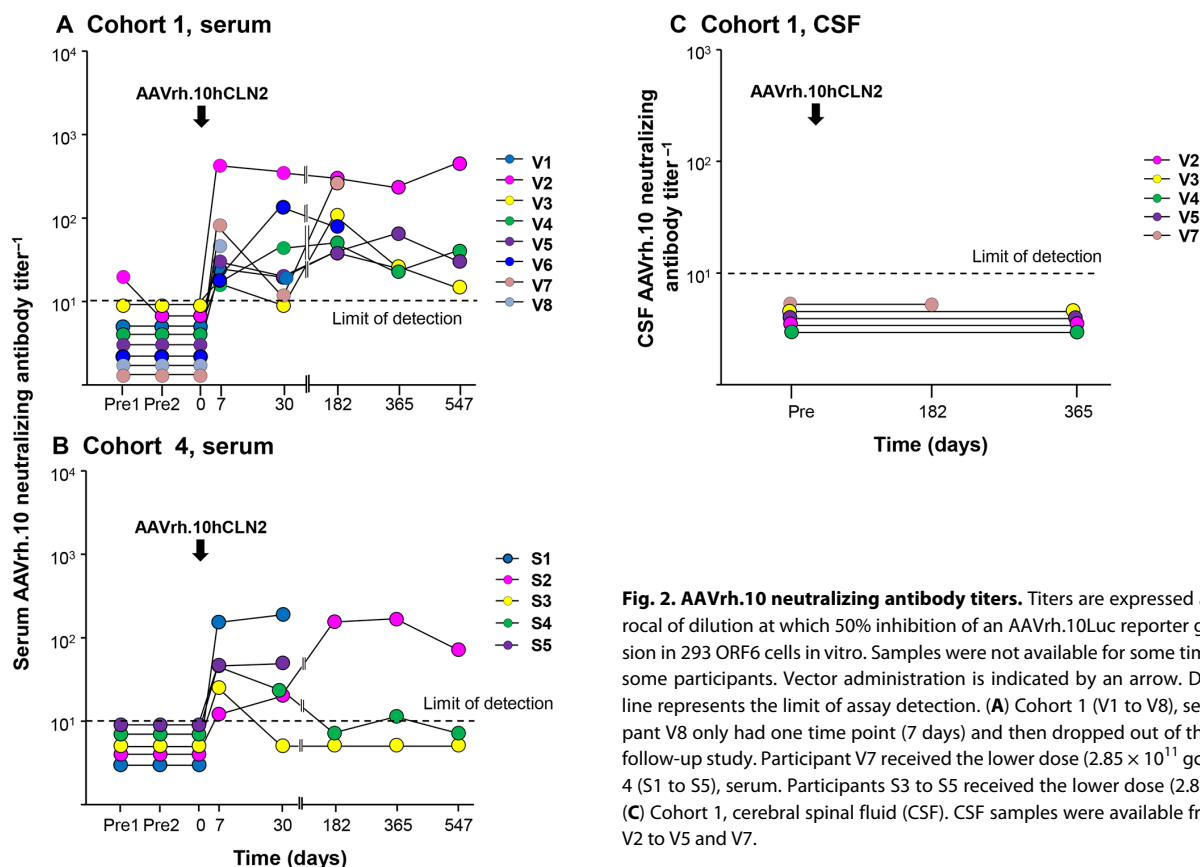


Fig. 2. AAVrh.10 neutralizing antibody titers. Titers are expressed as the reciprocal of dilution at which 50% inhibition of an AAVrh.10Luc reporter gene expression in 293 ORF6 cells in vitro. Samples were not available for some time points for some participants. Vector administration is indicated by an arrow. Dashed black line represents the limit of assay detection. (A) Cohort 1 (V1 to V8), serum. Participant V8 only had one time point (7 days) and then dropped out of the 18-month follow-up study. Participant V7 received the lower dose (2.85×10^{11} gc). (B) Cohort 4 (S1 to S5), serum. Participants S3 to S5 received the lower dose (2.85×10^{11} gc). (C) Cohort 1, cerebral spinal fluid (CSF). CSF samples were available from subjects V2 to V5 and V7.

two eyes (38, 39). This retinal degeneration ultimately results in widespread retinal atrophy encompassing the entire fundus. None of the eyes of the CLN2 subjects exhibited any anterior segment abnormalities, regardless of the severity of the retinal degeneration, the advancing age of the subjects, or the extent of neurological deterioration.

One subject (V3) evaluated before CNS-directed gene therapy at age 53 months was found to have a central macular thickness (CMT) in the right eye of 295 μm and in the left eye of 282 μm . Seven months after CNS-directed CLN2 gene therapy, at age 60 months, the CMT of the right eye was 266 μm , and CMT of the left eye was 267 μm : Despite the CNS gene therapy, the ophthalmic degeneration in both eyes followed the same accelerated decline as was seen with the natural history of untreated patients. The progressive retinal changes noted on exam and on dilated fundus photography in all eyes demonstrated continued degeneration despite the CNS-directed gene therapy.

The primary efficacy parameter was the neurologic rating scale of assessment of motor + language. The reproducibility of the measurement of the motor and language parameters demonstrated an average coefficient of variation among the assessors of 0.07 ± 0.14 for the motor domain and 0.16 ± 0.18 for the language domain (table S7). To determine the reproducibility of the motor + language assessment, based on the knowledge that our primary rating scale should not change in a short period, we assessed data from $n = 6$ children that had repeat assessments <1.5 months apart. The data demonstrated excellent reproducibility in the repeat assessments of the subjects for motor ($P > 0.9$), language ($P > 0.6$), and for the combined score of motor and language ($P > 0.7$; table S8).

The consensus motor + language neurologic parameter of the therapy/safety and efficacy group (cohort 1; table 2) was compared with the Weill Cornell natural history control cohort (cohort 2; table S9) and to the European DEM Child Natural History Replication (cohort 3) datasets (Fig. 5). The difference in the annual rate of decline between the two control groups was not significant ($P > 0.2$). In contrast, the decline per year in the treated subjects was slower in comparison to the decline for both control groups. The annual rate of decline for the treated cohort (cohort 1) was -0.95 ± 0.67 (means \pm SD, $n = 7$). In comparison, the annual rate of decline for the control cohort (cohort 2) was -1.65 ± 0.64 (means \pm SD, $n = 12$). The treatment yielded a 42.4% slowing in the rate of decline in motor + language assessment of treated to untreated children, which was statistically significant ($P < 0.04$). For the replication untreated European cohort (cohort 3), the annualized rate of decline was -1.81 ± 0.31 (means \pm SD, $n = 41$). Comparison of the treated group (cohort 1) to cohort 3 demonstrated a 47.5% slowing in the rate of decline ($P < 0.0001$).

Because of the small study population, it was not possible to reach definitive conclusions regarding the response to therapy of the different genotypes or age of treatment. With this caveat, as this information may be useful for the design of a larger study, we are presenting the data. There was no correlation between the annual rate of decline and the genotype of the treated subjects (fig. S9A) or between the age at vector administration and the rate of decline after treatment (fig. S9B). Similarly, assessment of impact of the motor + language score at the time of vector administration on the rate of decline did not demonstrate a correlation (fig. S9C). Last, we

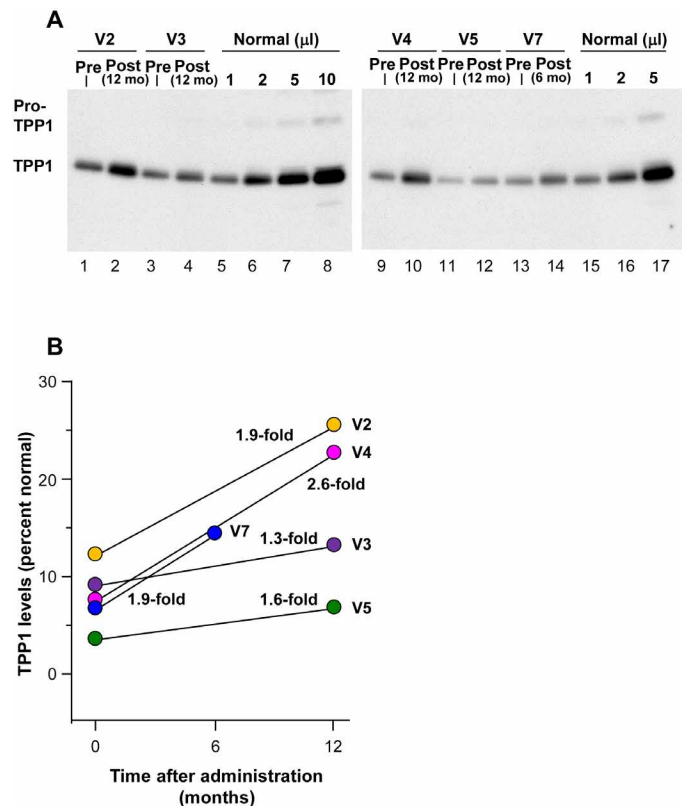


Fig. 3. Human TPP1 in CSF after AAVrh.10hCLN2 administration to cohort 1. CSF was analyzed for TPP1 by Western analysis. The Institutional Review Board-approved protocol allowed for CSF sampling before therapy and only one time after therapy. **(A)** Western analysis. Lanes 1 and 2, participant V2; lanes 3 and 4, participant V3; lanes 5 to 8, 1, 2, 5, and 10 μ l, respectively, of combined CSFs of three healthy children (1:1:1 volume mix) as a positive control. Lanes 9 and 10, participant V4; lanes 11 and 12, participant V5; lanes 13 and 14, participant V7; lanes 15 to 17, 1, 2, and 5 ml, respectively, of combined CSFs of three healthy subjects (1:1:1 volume mix) as a positive control. **(B)** Quantitation of TPP1 in CSF before and after therapy expressed as percent normal TPP1 in CSF after AAVrh.10hCLN2 administration compared to pre-administration (pre- versus post-percentage normal, $P < 0.03$, paired two-tailed t test). V7 received the lower dose (2.85×10^{11} gc).

evaluated the impact of the peak neutralizing antibody response after vector administration and its impact on the rate of decline; there was no correlation among these parameters (fig. S9D). The subject who had the highest systemic anti-AAVrh.10 neutralizing capsid antibody response (V2) had the best clinical response with the resulting rate of motor + language decline of -0.3 units/year.

In a study carried out by BioMarin Pharmaceuticals, with bi-weekly intraventricular infusions of cerliponase alfa (recombinant TPP1) in 23 subjects, the mean (\pm SD) rate of decline using the same motor + language score per 48-week period was -0.27 ± 0.35 in treated patients (31), extrapolated to an annual rate of decline of -0.29 ± 0.38 . Compared to the natural history control groups, this represents an improvement of 82.4 to 84.0% in slowing the rate of decline, compared to our gene therapy improvement of 42.4 to 47.5%.

DISCUSSION

In the present study, we used direct CNS administration of a serotype AAVrh.10 gene transfer vector to deliver the normal coding sequence of human CLN2 to the CNS of children with CLN2 disease.

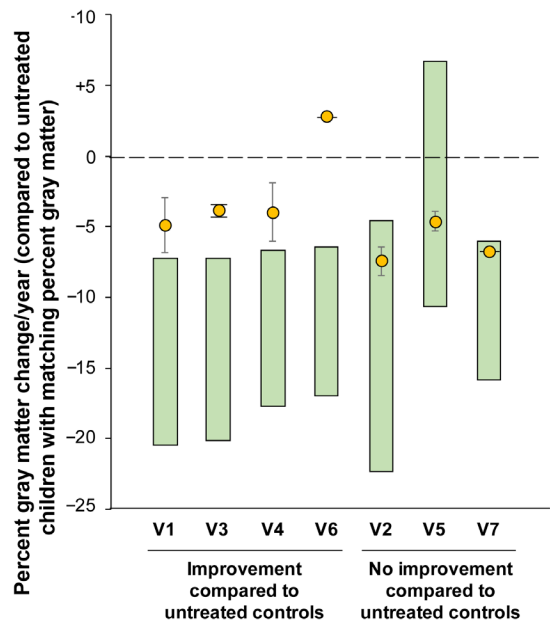


Fig. 4. Quantitative MRI assessment of gray matter decline in treated versus untreated CLN2 children. The reduction in the percent gray matter, assessed by MRI, is shown for each treated participant (yellow circle) above the range of gray matter decline (green bar) for untreated CLN2 children matched by percent gray matter. The range of the gray matter decline is derived from the data in figs. S5 and S6. Treated children with gray matter decline above the range for the untreated cohort indicates a decline that is slower and outside the 95% CI for untreated children. Participants V2 and V5 were the youngest trial participants and had slow rates of decline at the time of treatment such that the effect of therapy was not yet apparent. Participant V6 had only one posttreatment scan, and therefore, error bars could not be calculated. Participant V7 received the lower dose (2.85×10^{11} gc).

The administration of the vector and subsequent follow-up over 18 months demonstrated that the therapy was safe, with minimal serious adverse events, and presented preliminary measures of efficacy. The challenges of testing the gene therapy for CLN2 disease include the highly variable clinical phenotype in a relatively small target population that makes statistically relevant conclusions difficult. Furthermore, the complex arrays of clinical sequelae that include seizures, motor neuron dysfunction, and cognitive impairment, which differ among individuals, create a barrier to evaluating safety as well.

The current U.S.- and Europe-approved treatment option for the CNS manifestations of CLN2 disease is recombinant TPP1 administered every other week via a subcutaneous reservoir with a catheter into a CNS ventricle (30–32). Although AAVrh.10hCLN2 therapy slowed progression of the CNS disease, using the same control group (the European DEM Child Natural History Replication Control Cohort) as the comparator, recombinant TPP1 therapy was more efficacious, with a greater reduction in the rate of decline of the same neurologic parameters compared to gene therapy. Recombinant TPP1 therapy provided an 84.0% decrease in the rate of neurological decline, compared to 47.5% for this gene therapy. If the gene therapy could be improved, the theoretical advantage is that it could potentially be efficacious with a single administration, whereas the recombinant TPP1 therapy requires administration every other week (31, 40, 41). Gene therapy would also substantially reduce the costs over a lifetime and assure 100% compliance.

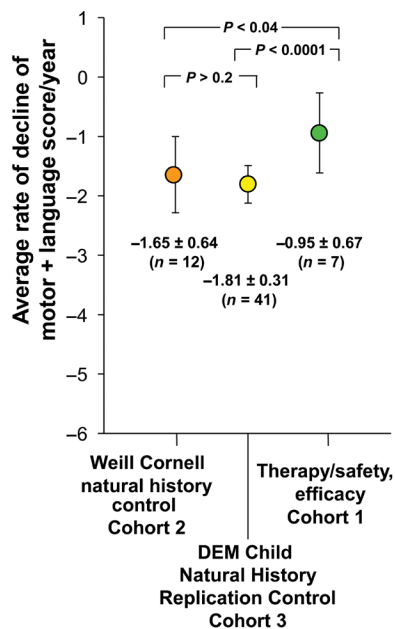


Fig. 5. Quantitation of the rate of decline of motor and language assessment in the therapy cohort (cohort 1) compared to Weill Cornell natural history control cohort (cohort 2) and the DEM Child Natural History Replication Control cohort (cohort 3). For cohorts 1 and 2, linear regression was taken for each participant's motor and language assessment over time to calculate the individual rate of decline. The individual rates of decline for all children within a cohort were then averaged to calculate the rate of decline per year for each individual cohort. The rates of decline per year for each cohort are plotted as a mean rate of decline with the error bars representing ± 1 SD from the mean. The raw data for cohorts 1 and 3 are in Table 2 and table S7. For cohort 3, the sample size, mean, and SD were derived from (5); *P* values were determined using a two-tailed unpaired Student's *t* test.

There are several approaches to improve the gene therapy. First would be to combine the direct parenchymal administration route with additional routes such as intracerebroventricular and/or intracisternal delivery, which have also been shown to lead to widespread distribution of transgene products (42–47). TPP1 is a secreted protein and is capable of cross-correcting neighboring cells mediated via the mannose-6-receptor pathway (27–29). It is not necessary to transfer the normal *CLN2* cDNA to all of the cells in the CNS; corrected cells will secrete TPP1, which is then endocytosed via the mannose-6-phosphate receptor pathway by neighboring cells for therapeutic correction (12, 28). AAV-based gene therapy, which would be unlikely to transduce every cell with the normal therapeutic gene, is the source of corrective enzymes for even the noninfected neighboring cells, and thus, additional routes of administrations may provide a greater potential for the success of the therapy (12, 28, 46). To inform future clinical development of AAVrh.10hCLN2, we are planning nonhuman primate studies of direct comparison of the distribution of vector expression by each of the different routes of administration or in combination. Second, an alternative approach would be to combine the intraparenchymal gene therapy strategy together with recombinant TPP1, likely leading to greater efficacy and possibly reducing the frequency of administration and/or dose of recombinant TPP1 to achieve maximal efficacy.

Third, we chose the AAVrh.10 vector based on effective experimental animal studies in rodents and nonhuman primates (33–35). Although the AAVrh.10hCLN2 vector was efficacious in slowing

the rate of progression of the disease, it is possible that improvements in vector and/or expression cassette design could provide better distribution and higher concentrations of TPP1 throughout the brain.

Fourth, despite the fact that no immunosuppression was used in the current study, there was little evidence of systemic anti-capsid neutralizing antibodies or anti-capsid/anti-transgene cellular immunity generated by the CNS gene therapy. No subjects had evidence of inflammation in CSF. Most had CNS MRI lesions localized to the region at the tip of the catheter. While CNS antivector immunity could lead to lack of efficacy, all of the subjects assessed had increased expression of TPP1 in the CSF 6 months to 1 year after administration, and there was no capsid anti-neutralizing antibody in the CSF. The lack of anti-capsid neutralizing antibodies in the CSF suggests that readministration of the gene therapy vector could be used to boost the response.

Fifth, the dose could be increased. Although this is unlikely to be safe with intraparenchymal administration, it might be done by the intracerebroventricular or intracisternal routes.

Last, in the children screened, the average time from the first symptom to diagnosis of CLN2 disease was 19 months. Anecdotally, the youngest treated child had the best reduction in slowing of the rate of decline on the neurologic rating scale, and studies in murine knockout model of CLN2 disease demonstrated that earlier treatment is more effective (35, 48). In this context, it is likely that there would be improvement in efficacy with earlier diagnosis and treatment.

In conclusion, direct intraparenchymal AAVrh.10hCLN2 vector administration is safe, and there is a therapeutic benefit over 18 months, slowing the rate of neurological decline from CLN2 disease. However, although direct comparisons have not been made, compared to the same control group, the gene therapy is not as effective as recombinant TPP1 therapy administered biweekly. This provides the rationale for developing future clinical trials of AAV gene transfer in children with CLN2 disease using more effective CNS delivery strategies, consideration of immunotherapy, and possibility of higher doses. To achieve maximal effectiveness, gene therapy for CLN2 disease should begin early, ideally before symptom onset. This will require earlier diagnosis and emphasizes the importance of adding CLN2 disease to universal newborn screening.

MATERIALS AND METHODS

Study design

The goal of this study was to assess the safety and preliminary efficacy of intraparenchymal delivery of AAVrh.10hCLN2 in a nonrandomized trial consisting of two cohorts assessed over 18 months: cohort 1 (mild to moderate neurologic disease, treated with AAVrh.10hCLN2) and cohort 2 (mild to moderate disease, no therapy; Food and Drug Administration (FDA) BB IND13591; ClinicalTrials.gov identifiers: NCT01035424 and NCT01161576; Table 1). As per the inclusion/exclusion criteria (table S10), the genotype of each subject had to include at least one of the five following *CLN2* mutant genotypes: C3670T (nonsense Arg²⁰⁸ to stop), G3556C (intron 7 splice), G5271C (Gln⁴²²His), T4396G (aberrant splicing, intron 8), and G4655A (Cys³⁶⁵Tyr) (1, 2, 5, 11). If either parental allele was R447H (Arg⁴⁴⁷His, a known “slow progression” genotype), the subject was not included (11, 49, 50). Before therapy, all children had confirmation of their *CLN2* mutations, routine blood and urine studies, comprehensive neurological assessments (CNS MRI and neurologic rating scale),

assessment of anti-AAVrh.10 neutralizing antibodies, and assessment of relative quantity (before/after) of TPP1 in the CSF. Cohort 1 included $n = 8$ children (V1 to V8), and cohort 2 included $n = 12$ children (C1 to C12).

Cohort 1 received 2.85×10^{11} to 9.0×10^{11} gc of AAVrh.10hCLN2 (six received 9.0×10^{11} gc, and two received 2.85×10^{11} gc) delivered directly via catheter into the CNS via six burr holes (three bilaterally), with equal doses to two sites per burr hole (51–53). No immunosuppression was used. One child (V8) did not return for any follow-up visit in the 18-month study and was excluded from the analysis of efficacy parameters.

The primary efficacy parameter was a CLN2 neurologic rating scale assessing motor and language parameters (table S1). As a replication control cohort for the CLN2 neurologic rating scale, comparison was also made to cohort 3 (Table 1), a control cohort from the published European CLN2 neurologic rating scale DEM Child Natural History study of $n = 41$ untreated children with CLN2 disease followed longitudinally for an average of 28 assessments over the life of the child (5). Details regarding cohort 3 are in (5). Secondary efficacy parameters included assessment of TPP1 in CSF and MRI assessment of percent gray matter volume. For comparison of the MRI percent gray matter volume of the treated children, the control data included data from $n = 62$ MRI obtained from 47 children with CLN2 disease, including the untreated controls (cohort 2), the pretherapy time points for the children in cohorts 1 and 4, and children in the screening study that did not participate in the therapy versus no-therapy study. Additional secondary efficacy parameters included parental assessment using the Child Health Questionnaire (CHQ) or Infant Toddler Quality of Life (ITQoL) quality of life questionnaire (depending on age) and the Mullen scale. See below for details regarding the efficacy parameters, table S10 for inclusion/exclusion criteria for cohorts 1 and 2, and table S11 for the timeline for cohorts 1 and 2.

The safety data also included cohort 4, a therapy/safety-only cohort of $n = 5$ children who were not eligible for the “therapy versus no-therapy” study based on disease severity and/or genotype (see table S12 for inclusion/exclusion criteria for cohort 4). Cohort 4 was treated with AAVrh.10hCLN2 in the identical fashion as cohort 1, with $n = 2$ at 9.0×10^{11} gc total dose divided into 12 sites and $n = 3$ at 2.85×10^{11} gc total dose. The timeline for cohort 4 was similar to that of cohort 1 (table S11). Because the children did not fit the eligibility criteria for the therapy versus no-therapy study, the data were only used for safety comparisons. No immunosuppression was used. Detailed methods regarding AAVrh.10hCLN2 administration and post-administration assessments including safety and efficacy parameters are provided in Supplementary Materials and Methods.

AAVrh.10hCLN2

AAVrh.10hCLN2 is composed of the capsid of AAVrh.10, a clade E AAV derived from rhesus macaque (33, 54, 55) and a genome composed of 5' and 3' AAV2 inverted terminal repeats surrounding an expression cassette including the following: the enhancer from human cytomegalovirus; promoter, splice donor, and left-hand intron sequence from chicken β -actin (CAG); the splice acceptor from rabbit β -globin; the normal human CLN2 coding sequence cDNA; and the rabbit β -globin polyadenylation sequence (fig. S1) (34, 56). AAVrh.10hCLN2 was produced by a two-plasmid cotransfection under Good Manufacturing Practice conditions at the Belfer Gene Therapy Core Facility,

Weill Cornell Medical College. This cotransfection of an expression cassette plasmid (pAAV2-CAG-hCLN2) and an adenovirus/AAVrh.10 helper plasmid (pPAK-MArh.10) was carried out in a certified 293T cell line using PolyFect reagent (Qiagen Sciences). The helper plasmid included the AAVrh.10 cap gene and AAV2 rep gene necessary for viral reproduction and capsid production. The vector was released from cells after three freeze-thaw cycles 72 hours after transfection, and a crude viral lysate (CVL) was generated. Benzonase (Sigma-Aldrich) was used to remove any contaminant genomic DNA. The remaining CVL was centrifuged, and the supernatant was applied to a discontinuous iodixanol gradient, and then purified by Q-HP ion exchange chromatography, and centrifugally concentrated into phosphate-buffered saline (pH 7.4). Vector concentration in gc was determined by TaqMan real-time polymerase chain reaction. To confirm functionality, human embryonic kidney 293-ORF6 cells were infected with AAVrh.10hCLN2, and TPP1 enzymatic activity was verified in the cell supernatant 72 hours after infection (33, 57). Full characterization of the final product included U.S. FDA-approved lot release assays to ensure identity, purity, and function.

Statistical analysis

Association of postoperative T2 FLAIR, ADC, or DWI with dose was performed by a two-tailed Fisher's exact test. For the Mullen scale and CHQs, data were analyzed using a two-tailed unpaired Student's t test. In the assessment of the primary efficacy parameter, the CLN2 neurologic rating scale, the P value was calculated using a standard t test assuming equal variance. For cohort 3, the sample size, mean, and SD were derived from Nickel *et al.* (5); a two-tailed unpaired Student's t test was used to compare cohort 1 and cohort 2 individually against cohort 3.

SUPPLEMENTARY MATERIALS

stm.sciencemag.org/cgi/content/full/12/572/eabb5413/DC1

Materials and Methods

Fig. S1. AAVrh.10hCLN2 vector.

Fig. S2. Trajectory planning for gene therapy infusions.

Fig. S3. Axial T2 FLAIR (T2 FLAIR) assessment of participants after therapy.

Fig. S4. T cell responses to AAVrh.10 capsid and CLN2 transgene.

Fig. S5. MRI assessment of the treated CLN2 children versus untreated CLN2 children.

Fig. S6. Quantitative MRI assessment of the treated CLN2 children (cohort 1) versus untreated CLN2 children.

Fig. S7. Mullen scale quantitation of the rate of decline for cohorts 1 (red, treated) and 2 (blue, control).

Fig. S8. Impact of treatment on quality of life as assessed by age-dependent quality of life questionnaires.

Fig. S9. Correlation of various parameters to the rate of decline of motor + language of cohort 1.

Table S1. CLN2 disease severity clinical rating scales.

Table S2. Vector infusion time and operating room surgery and anesthesia duration in cohort 1 participants.

Table S3. Vector infusion time and operating room surgery and anesthesia duration in cohort 4 participants.

Table S4. CSF nucleated cells.

Table S5. Percent volume of the brain with MRI T2 hyperintensity.

Table S6. Quality of life questionnaires.

Table S7. Coefficient of variation among observers in the CLN2 disease motor + language neurologic rating scale.

Table S8. Reproducibility of motor and language assessment.

Table S9. Assessments of motor and language parameters for cohort 2.

Table S10. Inclusion/exclusion criteria for cohorts 1 and 2.

Table S11. Timeline of the clinical study.

Table S12. Inclusion/exclusion criteria for cohort 4.

References (58–68)

[View/request a protocol for this paper from Bio-protocol.](#)

REFERENCES AND NOTES

- D. E. Sleat, R. J. Donnelly, H. Lackland, C. G. Liu, I. Sohar, R. K. Pullarkat, P. Lobel, Association of mutations in a lysosomal protein with classical late-infantile neuronal ceroid lipofuscinosis. *Science* **277**, 1802–1805 (1997).
- R. E. Williams, I. Gottlob, B. D. Lake, H. H. Goebel, W. Wheeler, R. B. Wheeler, in *The Neuronal Ceroid Lipofuscinoses (Batten Disease)*, H. H. Goebel, S. E. Mole, B. D. Lake, Eds. (IOS Press, 1999), pp. 37–54.
- M. Haltia, The neuronal ceroid-lipofuscinoses. *J. Neuropathol. Exp. Neurol.* **62**, 1–13 (2003).
- S. Worgall, M. V. Kekatpure, L. Heier, D. Ballon, J. P. Dyke, D. Shungu, X. Mao, B. Kosofsky, M. G. Kaplitt, M. M. Souweidane, D. Sondhi, N. R. Hackett, C. Hollmann, R. G. Crystal, Neurological deterioration in late infantile neuronal ceroid lipofuscinosis. *Neurology* **69**, 521–535 (2007).
- M. Nickel, A. Simonati, D. Jacoby, S. Lezius, D. Kilian, B. Van de Graaf, O. E. Pagovich, B. Kosofsky, K. Yohay, M. Downs, P. Slasor, T. Ajayi, R. G. Crystal, A. Kohlschutter, D. Sondhi, A. Schulz, Disease characteristics and progression in patients with late-infantile neuronal ceroid lipofuscinosis type 2 (CLN2) disease: An observational cohort study. *Lancet Child Adolesc. Health* **2**, 582–590 (2018).
- D. Rakheja, M. J. Bennett, Neuronal ceroid-lipofuscinoses. *Transl. Sci. Rare Dis.* **3**, 83–95 (2018).
- M. Fietz, M. AlSayed, D. Burke, J. Cohen-Pfeffer, J. D. Cooper, L. Dvorakova, R. Giugliani, E. Izzo, H. Jahnova, Z. Lukacs, S. E. Mole, I. Noher de Halac, D. A. Pearce, H. Poupetova, A. Schulz, N. Specchio, W. Xin, N. Miller, Diagnosis of neuronal ceroid lipofuscinosis type 2 (CLN2 disease): Expert recommendations for early detection and laboratory diagnosis. *Mol. Genet. Metab.* **119**, 160–167 (2016).
- R. E. Williams, H. R. Adams, M. Blohm, J. L. Cohen-Pfeffer, E. de Los Reyes, J. Denecke, K. Drago, C. Fairhurst, M. Frazier, N. Guelbert, S. Kiss, A. Kofler, J. A. Lawson, L. Lehwald, M. A. Leung, S. Mikhaylova, J. W. Mink, M. Nickel, R. Shediak, K. Sims, N. Specchio, M. Topcu, I. von Lobbecke, A. West, B. Zernikow, A. Schulz, Management strategies for CLN2 disease. *Pediatr. Neurol.* **69**, 102–112 (2017).
- A. Jalanko, T. Braulke, Neuronal ceroid lipofuscinoses. *Biochim. Biophys. Acta* **1793**, 697–709 (2009).
- S. E. Mole, M. Haltia, in *Rosenberg's Molecular and Genetic Basis of Neurological and Psychiatric Disease*, R. N. Rosenberg, J. M. Pascual, Eds. (Academic Press, 2015), chap. 70, p. 16.
- E. Gardner, M. Bailey, A. Schulz, M. Aristorena, N. Miller, S. E. Mole, Mutation update: Review of *TPP1* gene variants associated with neuronal ceroid lipofuscinosis CLN2 disease. *Hum. Mutat.* **40**, 1924–1938 (2019).
- D. Sondhi, N. R. Hackett, R. L. Apblett, S. M. Kaminsky, R. G. Pergolizzi, R. G. Crystal, Feasibility of gene therapy for late neuronal ceroid lipofuscinosis. *Arch. Neurol.* **58**, 1793–1798 (2001).
- D. Sondhi, J. B. Rosenberg, B. Van de Graaf, S. M. Kaminsky, R. G. Crystal, Advances in the treatment of neuronal ceroid lipofuscinosis. *Expert Opin. Orphan Drugs* **1**, 951–975 (2013).
- M. A. Tarczyluk, J. D. Cooper, Investigative and emerging treatments for Batten disease. *Expert Opin. Orphan Drugs* **3**, 1031–1045 (2015).
- A. Donsante, N. M. Boulis, Progress in gene and cell therapies for the neuronal ceroid lipofuscinoses. *Expert Opin. Biol. Ther.* **18**, 755–764 (2018).
- A. Kohlschutter, A. Schulz, U. Bartsch, S. Storch, Current and emerging treatment strategies for neuronal ceroid lipofuscinoses. *CNS Drugs* **33**, 315–325 (2019).
- T. B. Johnson, J. T. Cain, K. A. White, D. Ramirez-Montealegre, D. A. Pearce, J. M. Weimer, Therapeutic landscape for Batten disease: Current treatments and future prospects. *Nat. Rev. Neurol.* **15**, 161–178 (2019).
- S. E. Mole, G. Anderson, H. A. Band, S. F. Berkovic, J. D. Cooper, S. M. Kleine Holthaus, T. R. McKay, D. L. Medina, A. A. Rahim, A. Schulz, A. J. Smith, Clinical challenges and future therapeutic approaches for neuronal ceroid lipofuscinosis. *Lancet Neurol.* **18**, 107–116 (2019).
- J. B. Rosenberg, A. Chen, S. M. Kaminsky, R. G. Crystal, D. Sondhi, Advances in the treatment of neuronal ceroid lipofuscinosis. *Expert Opin. Orphan Drugs*, 473–500 (2019).
- S. J. Gray, Gene therapy and neurodevelopmental disorders. *Neuropharmacology* **68**, 136–142 (2013).
- M. S. Weinberg, R. J. Samulski, T. J. McCown, Adeno-associated virus (AAV) gene therapy for neurological disease. *Neuropharmacology* **69**, 82–88 (2013).
- M. Hocquemiller, L. Giersch, M. Audrain, S. Parker, N. Cartier, Adeno-associated virus-based gene therapy for CNS diseases. *Hum. Gene Ther.* **27**, 478–496 (2016).
- G. Murlidharan, R. J. Samulski, A. Asokan, in *Translational Neuroscience Fundamental Approaches for Neurological Disorders*, M. H. Tuszynski, Ed. (Springer, 2016), chap. 2, p. 24.
- B. E. Deverman, B. M. Ravina, K. S. Bankiewicz, S. M. Paul, D. W. Y. Sah, Gene therapy for neurological disorders: Progress and prospects. *Nat. Rev. Drug Discov.* **17**, 641–659 (2018).
- E. Hudry, L. H. Vandenbergh, Therapeutic AAV gene transfer to the nervous system: A clinical reality. *Neuron* **101**, 839–862 (2019).
- D. E. Sleat, R. M. Gin, I. Sohar, K. Wisniewski, S. Sklower-Brooks, R. K. Pullarkat, D. N. Palmer, T. J. Lerner, R. M. Boustany, P. Uldall, A. N. Siakotos, R. J. Donnelly, P. Lobel, Mutational analysis of the defective protease in classic late-infantile neuronal ceroid lipofuscinosis, a neurodegenerative lysosomal storage disorder. *Am. J. Hum. Genet.* **64**, 1511–1523 (1999).
- E. F. Neufeld, J. C. Fratantoni, Inborn errors of mucopolysaccharide metabolism. *Science* **169**, 141–146 (1970).
- D. Sondhi, R. G. Crystal, S. M. Kaminsky, in *Translational Neuroscience Fundamental Approaches For Neurological Disorders*, M. H. Tuszynski, Ed. (Springer, 2016), chap. 7, p. 19.
- F. M. Platt, A. d'Azzo, B. L. Davidson, E. F. Neufeld, C. J. Tiff, Lysosomal storage diseases. *Nat. Rev. Dis. Primers.* **4**, 27 (2018).
- A. Markham, Cerliponase alfa: First global approval. *Drugs* **77**, 1247–1249 (2017).
- A. Schulz, T. Ajayi, N. Specchio, E. de Los Reyes, P. Gissen, D. Ballon, J. P. Dyke, H. Cahan, P. Slasor, D. Jacoby, A. Kohlschutter; CLN2 Study Group, Study of intravitreal cerliponase alfa for CLN2 disease. *N. Engl. J. Med.* **378**, 1898–1907 (2018).
- A. Schulz, N. Specchio, P. Gissen, E. De Los Reyes, H. Cahan, P. Slasor, D. Jacoby, T. Ajayi, Persistent treatment effect of cerliponase alfa in children with CLN2 disease: A 3 year update from an ongoing multicenter extension study. *Neuropediatrics* **50**, S1–S55 (2019).
- D. Sondhi, N. R. Hackett, D. A. Peterson, J. Stratton, M. Baad, K. M. Travis, J. M. Wilson, R. G. Crystal, Enhanced survival of the LINCL mouse following CLN2 gene transfer using the rh.10 rhesus macaque-derived adeno-associated virus vector. *Mol. Ther.* **15**, 481–491 (2007).
- D. Sondhi, L. Johnson, K. Purpura, S. Monette, M. M. Souweidane, M. G. Kaplitt, B. Kosofsky, K. Yohay, D. Ballon, J. Dyke, S. M. Kaminsky, N. R. Hackett, R. G. Crystal, Long-term expression and safety of administration of AAVrh.10hCLN2 to the brain of rats and nonhuman primates for the treatment of late infantile neuronal ceroid lipofuscinosis. *Hum. Gene Ther. Methods* **23**, 324–335 (2012).
- D. Sondhi, D. A. Peterson, A. M. Edelstein, K. del Fierro, N. R. Hackett, R. G. Crystal, Survival advantage of neonatal CNS gene transfer for late infantile neuronal ceroid lipofuscinosis. *Exp. Neurol.* **213**, 18–27 (2008).
- J. P. Dyke, D. Sondhi, H. U. Voss, D. C. Shungu, X. Mao, K. Yohay, S. Worgall, N. R. Hackett, C. Hollmann, M. E. Yeotsas, A. L. Jeong, B. Van de Graaf, I. Cao, S. M. Kaminsky, L. A. Heier, K. D. Rudser, M. M. Souweidane, M. G. Kaplitt, B. Kosofsky, R. G. Crystal, D. Ballon, Assessment of disease severity in late infantile neuronal ceroid lipofuscinosis using multiparametric MR imaging. *AJNR Am. J. Neuroradiol.* **34**, 884–889 (2013).
- J. P. Dyke, D. Sondhi, H. U. Voss, K. Yohay, C. Hollmann, D. Mancenido, S. M. Kaminsky, L. A. Heier, K. D. Rudser, B. Kosofsky, B. J. Casey, R. G. Crystal, D. Ballon, Brain region-specific degeneration with disease progression in late infantile neuronal ceroid lipofuscinosis (CLN2 Disease). *AJNR Am. J. Neuroradiol.* **37**, 1160–1169 (2016).
- K. D. Kovacs, S. Patel, A. Orlin, K. Kim, S. Van Everen, T. Conner, D. Sondhi, S. M. Kaminsky, D. J. D'Amico, R. G. Crystal, S. Kiss, Symmetric age association of retinal degeneration in patients with CLN2-associated Batten disease. *Ophthalmol. Retina* **4**, 728–736 (2020).
- A. Orlin, D. Sondhi, M. T. Witmer, M. M. Wessel, J. G. Mezey, S. M. Kaminsky, N. R. Hackett, K. Yohay, B. Kosofsky, M. M. Souweidane, M. G. Kaplitt, D. J. D'Amico, R. G. Crystal, S. Kiss, Spectrum of ocular manifestations in CLN2-associated batten (Jansky-Bielschowsky) disease correlate with advancing age and deteriorating neurological function. *PLOS ONE* **8**, e73128 (2013).
- F. Zairi, E. Le Rhun, N. Bertrand, T. Boulanger, S. Taillibert, R. Aboukais, R. Assaker, M. C. Chamberlain, Complications related to the use of an intravitreal access device for the treatment of leptomeningeal metastases from solid tumor: A single centre experience in 112 patients. *J. Neurooncol.* **124**, 317–323 (2015).
- I. Slavic, J. L. Cohen-Pfeffer, S. Gururangan, J. Krauser, D. A. Lim, M. Maldaun, C. Schwering, A. J. Shaywitz, M. Westphal, Best practices for the use of intracerebroventricular drug delivery devices. *Mol. Genet. Metab.* **124**, 184–188 (2018).
- S. J. Gray, S. Nagabhushan Kalburgi, T. J. McCown, R. Jude Samulski, Global CNS gene delivery and evasion of anti-AAV-neutralizing antibodies by intrathecal AAV administration in non-human primates. *Gene Ther.* **20**, 450–459 (2013).
- L. Samaranch, E. A. Salegio, W. San Sebastian, A. P. Kells, K. D. Foust, J. R. Bringas, C. Lamarre, J. Forsayeth, B. K. Kaspar, K. S. Bankiewicz, Adeno-associated virus serotype 9 transduction in the central nervous system of nonhuman primates. *Hum. Gene Ther.* **23**, 382–389 (2012).
- Y. Matsuzaki, A. Konno, R. Mukai, F. Honda, M. Hirato, Y. Yoshimoto, H. Hirai, Transduction profile of the marmoset central nervous system using adeno-associated virus serotype 9 vectors. *Mol. Neurobiol.* **54**, 1745–1758 (2017).
- J. Naidoo, L. M. Stanek, K. Ohno, S. Trewwan, L. Samaranch, P. Hadaczek, C. O'Riordan, J. Sullivan, W. San Sebastian, J. R. Bringas, C. Snieucus, A. Mahmoodi, A. Mahmoodi, J. Forsayeth, K. S. Bankiewicz, L. S. Shihabuddin, Extensive transduction and enhanced spread of a modified AAV2 Capsid in the non-human primate CNS. *Mol. Ther.* **26**, 2418–2430 (2018).
- J. B. Rosenberg, M. G. Kaplitt, B. P. De, A. Chen, T. Flagiello, C. Salami, E. Pey, L. Zhao, R. J. Ricart Arbona, S. Monette, J. P. Dyke, D. J. Ballon, S. M. Kaminsky, D. Sondhi, G. A. Petsko, S. M. Paul, R. G. Crystal, AAVrh.10-mediated APOE2 central nervous system

- gene therapy for APOE4-associated Alzheimer's disease. *Hum. Gene Ther. Clin. Dev.* **29**, 24–47 (2018).
47. M. L. Katz, L. Tecedor, Y. Chen, B. G. Williamson, E. Lysenko, F. A. Winger, W. M. Young, G. C. Johnson, R. E. Whiting, J. R. Coates, B. L. Davidson, AAV gene transfer delays disease onset in a TPP1-deficient canine model of the late infantile form of Batten disease. *Sci. Transl. Med.* **7**, 313ra180 (2015).
 48. M. A. Cabrera-Salazar, E. M. Roskelley, J. Bu, B. L. Hodges, N. Yew, J. C. Dodge, L. S. Shihabuddin, I. Sohar, D. E. Sleat, R. K. Scheule, B. L. Davidson, S. H. Cheng, P. Lobel, M. A. Passini, Timing of therapeutic intervention determines functional and survival outcomes in a mouse model of late infantile Batten disease. *Mol. Ther.* **15**, 1782–1788 (2007).
 49. L. Lin, P. Lobel, Expression and analysis of CLN2 variants in CHO cells: Q100R represents a polymorphism, and G389E and R447H represent loss-of-function mutations. *Hum. Mutat.* **18**, 165 (2001).
 50. M. Kousi, A. E. Lehesjoki, S. E. Mole, Update of the mutation spectrum and clinical correlations of over 360 mutations in eight genes that underlie the neuronal ceroid lipofuscinoses. *Hum. Mutat.* **33**, 42–63 (2012).
 51. R. G. Crystal, D. Sondhi, N. R. Hackett, S. M. Kaminsky, S. Worgall, P. Stieg, M. Souweidane, S. Hosain, L. Heier, D. Ballon, M. Dinner, K. Wisniewski, M. Kaplitt, B. M. Greenwald, J. D. Howell, K. Strybing, J. Dyke, H. Voss, Clinical protocol. Administration of a replication-deficient adeno-associated virus gene transfer vector expressing the human CLN2 cDNA to the brain of children with late infantile neuronal ceroid lipofuscinosis. *Hum. Gene Ther.* **15**, 1131–1154 (2004).
 52. S. Worgall, D. Sondhi, N. R. Hackett, B. Kosofsky, M. V. Kekatpure, N. Neyzi, J. P. Dyke, D. Ballon, L. Heier, B. M. Greenwald, P. Christos, M. Mazumdar, M. M. Souweidane, M. G. Kaplitt, R. G. Crystal, Treatment of late infantile neuronal ceroid lipofuscinosis by CNS administration of a serotype 2 adeno-associated virus expressing CLN2 cDNA. *Hum. Gene Ther.* **19**, 463–474 (2008).
 53. M. M. Souweidane, J. F. Fraser, L. M. Arkin, D. Sondhi, N. R. Hackett, S. M. Kaminsky, L. Heier, B. E. Kosofsky, S. Worgall, R. G. Crystal, M. G. Kaplitt, Gene therapy for late infantile neuronal ceroid lipofuscinosis: Neurosurgical considerations. *J. Neurosurg. Pediatr.* **6**, 115–122 (2010).
 54. G. P. Gao, M. R. Alvira, L. Wang, R. Calcedo, J. Johnston, J. M. Wilson, Novel adeno-associated viruses from rhesus monkeys as vectors for human gene therapy. *Proc. Natl. Acad. Sci. U.S.A.* **99**, 11854–11859 (2002).
 55. C. N. Cearley, J. H. Wolfe, Transduction characteristics of adeno-associated virus vectors expressing cap serotypes 7, 8, 9, and Rh10 in the mouse brain. *Mol. Ther.* **13**, 528–537 (2006).
 56. T. M. Daly, T. Okuyama, C. Vogler, M. E. Haskins, N. Muzyczka, M. S. Sands, Neonatal intramuscular injection with recombinant adeno-associated virus results in prolonged beta-glucuronidase expression in situ and correction of liver pathology in mucopolysaccharidosis type VII mice. *Hum. Gene Ther.* **10**, 85–94 (1999).
 57. L. Lin, P. Lobel, Production and characterization of recombinant human CLN2 protein for enzyme-replacement therapy in late infantile neuronal ceroid lipofuscinosis. *Biochem. J.* **357**, 49–55 (2001).
 58. B. P. De, A. Heguy, N. R. Hackett, B. Ferris, P. L. Leopold, J. Lee, L. Pierre, G. Gao, J. M. Wilson, R. G. Crystal, High levels of persistent expression of α 1-antitrypsin mediated by the nonhuman primate serotype rh.10 adeno-associated virus despite preexisting immunity to common human adeno-associated viruses. *Mol. Ther.* **13**, 67–76 (2006).
 59. W. W. Hauswirth, T. S. Aleman, S. Kaushal, A. V. Cideciyan, S. B. Schwartz, L. Wang, T. J. Conlon, S. L. Boye, T. R. Flotte, B. J. Byrne, S. G. Jacobson, Treatment of leber congenital amaurosis due to RPE65 mutations by ocular subretinal injection of adeno-associated virus gene vector: Short-term results of a phase I trial. *Hum. Gene Ther.* **19**, 979–990 (2008).
 60. Y. Zhang, M. Brady, S. Smith, Segmentation of brain MR images through a hidden Markov random field model and the expectation-maximization algorithm. *IEEE Trans. Med. Imaging* **20**, 45–57 (2001).
 61. S. M. Smith, Fast robust automated brain extraction. *Hum. Brain Mapp.* **17**, 143–155 (2002).
 62. O. Voevodskaya, A. Simmons, N. Nordenskjold, J. Kullberg, H. Ahlstrom, L. Lind, L.-O. Wahlund, E. M. Larsson, E. Westman; Alzheimer's Disease Neuroimaging Initiative, The effects of intracranial volume adjustment approaches on multiple regional MRI volumes in healthy aging and Alzheimer's disease. *Front. Aging Neurosci.* **6**, 264 (2014).
 63. R. Steinfeld, P. Heim, H. von Gregory, K. Meyer, K. Ullrich, H. H. Goebel, A. Kohlschütter, Late infantile neuronal ceroid lipofuscinosis: Quantitative description of the clinical course in patients with CLN2 mutations. *Am. J. Med. Genet.* **112**, 347–354 (2002).
 64. K. W. Wyrwich, A. Schulz, M. Nickel, P. Slasor, T. Ajayi, D. R. Jacoby, A. Kohlschütter, An adapted clinical measurement tool for the key symptoms of CLN2 disease. *JEMS* **6**, 1–7 (2018).
 65. E. M. Mullen, *Mullen Scales of Early Learning: AGS Edition* (American Guidance Service, 1995).
 66. N. Akshoomoff, Use of the Mullen Scales of Early Learning for the assessment of young children with autism spectrum disorders. *Child Neuropsychol.* **12**, 269–277 (2006).
 67. H. Raat, J. M. Landgraf, R. Oostenbrink, H. A. Moll, M. L. Essink-Bot, Reliability and validity of the Infant and Toddler Quality of Life Questionnaire (ITQOL) in a general population and respiratory disease sample. *Qual. Life Res.* **16**, 445–460 (2007).
 68. N. McCullough, J. Parkes, M. White-Koning, E. Beckung, A. Colver, Reliability and validity of the Child Health Questionnaire-PF-50 for European children with cerebral palsy. *J. Pediatr. Psychol.* **34**, 41–50 (2009).

Acknowledgments: We thank A. Mushlin (Healthcare Policy and Research, Weill Cornell Medicine) for discussions relating to the trial design, J. Greenfield (Department of Neurological Surgery, Weill Cornell Medicine) for surgical assistance, R. Calcedo and J. Wilson (Gene Therapy Program, University of Pennsylvania) for assistance with cellular immunity assays, and N. Mohamed for help in preparing this manuscript. **Funding:** This study was supported, in part, by NIH 1R01NS061848 (to R.G.C.), NIH U54NS065768 (to R.G.C.), and UL1 TR000457 and Nathan's Battle, Cures Within Reach (R.G.C.), Noah's Hope (to R.G.C.), and Hope4Bridget foundations (to R.G.C.). **Author contributions:** D.S., S.M.K., N.R.H., and R.G.C. participated in the design and/or interpretation of the reported experiments or results; D.S., J.B.R., A.C., B.V.d.G., O.E.P., B.P.D., B.K., K.Y., S.W., R.J.K., L.A.H., R.G.C., G.W.M., F.X., and S.M.K. participated in the acquisition and/or analysis of data—safety data; D.S., J.B.R., A.C., B.V.d.G., O.E.P., B.K., K.Y., S.W., and R.G.C. participated in the acquisition and/or analysis of data—neurological efficacy data; D.S., J.P.D., S.M.K., J.B.R., D.J.B., and R.G.C. participated in the acquisition and/or analysis of data—MRI efficacy data; S.K. participated in the acquisition and/or analysis of data—ophthalmology data; D.S., J.B.R., S.M.K., and R.G.C. participated in drafting and/or revising the manuscript; J.G.M. was primarily responsible for a particular, specialized role in the research—statistics; M.S. and M.K. were primarily responsible for a particular, specialized role in the research—neurosurgery planning and drug delivery; D.S., S.M.K., and N.R.H. were primarily responsible for a particular, specialized role in the research—drug preparation and handling; L.A.H. was primarily responsible for a particular, specialized role in the research—neurodiology/safety; J.P.D. and D.J.B. were primarily responsible for a particular, specialized role in the research—vector-related safety/efficacy assays; B.M.G. was primarily responsible for a particular, specialized role in the research—hospital stays and visits; G.W.M., D.M., F.X., and R.J.K. were primarily responsible for a particular, specialized role in the research—regulatory, quality assurance, and monitoring; D.S., S.M.K., and R.G.C. provided administrative, technical, or supervisory support. **Competing interests:** R.G.C. is a consultant to BioMarin, a biotechnology company that markets Brineura, a recombinant TPP1 enzyme used to treat CLN2 disease. BioMarin was not involved in this study. After study completion, the CLN2 program and AAVrh.10hCLN2, the gene therapy vector used in this study, were licensed by Cornell University to LEXEO Therapeutics, a gene therapy biotechnology company founded by R.G.C. LEXEO had no role, financial or otherwise, in the design, conduct, analysis, or write-up of this study. R.G.C., D.S., and S.M.K. hold equity in and are advisors to LEXEO. All other authors declare that they have no competing interests. **Data and materials availability:** All data associated with this study are present in the paper or the Supplementary Materials. The vector construct AAVrh.10hCLN2 can be provided to academic researchers via a material transfer agreement upon request to Cornell's Center for Technology Licensing at Weill Cornell Medical College.

Submitted 2 March 2020

Accepted 11 November 2020

Published 2 December 2020

10.1126/scitranslmed.abb5413

Citation: D. Sondhi, S. M. Kaminsky, N. R. Hackett, O. E. Pagovich, J. B. Rosenberg, B. P. De, A. Chen, B. Van de Graaf, J. G. Mezey, G. W. Mammen, D. Mancenido, F. Xu, B. Kosofsky, K. Yohay, S. Worgall, R. J. Kaner, M. Souweidane, B. M. Greenwald, M. Kaplitt, J. P. Dyke, D. J. Ballon, L. A. Heier, S. Kiss, R. G. Crystal, Slowing late infantile Batten disease by direct brain parenchymal administration of a rh.10 adeno-associated virus expressing CLN2. *Sci. Transl. Med.* **12**, eabb5413 (2020).

Supplementary Materials for

Slowing late infantile Batten disease by direct brain parenchymal administration of a rh.10 adeno-associated virus expressing *CLN2*

Dolan Sondhi, Stephen M. Kaminsky, Neil R. Hackett, Odelya E. Pagovich, Jonathan B. Rosenberg, Bishnu P. De, Alvin Chen, Benjamin Van de Graaf, Jason G. Mezey, Grace W. Mammen, Denesy Mancenido, Fang Xu, Barry Kosofsky, Kaleb Yohay, Stefan Worgall, Robert J. Kaner, Mark Souwedaine, Bruce M. Greenwald, Michael Kaplitt, Jonathan P. Dyke, Douglas J. Ballon, Linda A. Heier, Szilard Kiss, Ronald G. Crystal*

*Corresponding author. Email: geneticmedicine@med.cornell.edu

Published 2 December 2020, *Sci. Transl. Med.* **12**, eabb5413 (2020)
DOI: 10.1126/scitranslmed.abb5413

This PDF file includes:

Materials and Methods

Fig. S1. AAVrh.10hCLN2 vector.

Fig. S2. Trajectory planning for gene therapy infusions.

Fig. S3. Axial T2 FLAIR (T2 FLAIR) assessment of participants after therapy.

Fig. S4. T cell responses to AAVrh.10 capsid and CLN2 transgene.

Fig. S5. MRI assessment of the treated CLN2 children versus untreated CLN2 children.

Fig. S6. Quantitative MRI assessment of the treated CLN2 children (cohort 1) versus untreated CLN2 children.

Fig. S7. Mullen scale quantitation of the rate of decline for cohorts 1 (red, treated) and 2 (blue, control).

Fig. S8. Impact of treatment on quality of life as assessed by age-dependent quality of life questionnaires.

Fig. S9. Correlation of various parameters to the rate of decline of motor + language of cohort 1.

Table S1. CLN2 disease severity clinical rating scales.

Table S2. Vector infusion time and operating room surgery and anesthesia duration in cohort 1 participants.

Table S3. Vector infusion time and operating room surgery and anesthesia duration in cohort 4 participants.

Table S4. CSF nucleated cells.

Table S5. Percent volume of the brain with MRI T2 hyperintensity.

Table S6. Quality of life questionnaires.

Table S7. Coefficient of variation among observers in the CLN2 disease motor + language neurologic rating scale.

Table S8. Reproducibility of motor and language assessment.

Table S9. Assessments of motor and language parameters for cohort 2.

Table S10. Inclusion/exclusion criteria for cohorts 1 and 2.

Table S11. Timeline of the clinical study.

Table S12. Inclusion/exclusion criteria for cohort 4.

References (58–68)

Materials and Methods

AAVrh.10hCLN2 administration

All children receiving the vector were prepared for anesthesia and surgery in a standard fashion. Design of the sites for vector administration specifically for each child was carried out within 24 hr prior to vector administration using the Brainlab system for image-guided surgery (Brainlab) based on a pre-operative MRI scan with head sentinels. The burr holes were made at the pre-determined marked locations, the dura opened, and 150 μ m diameter flexible glass catheters (Polymicro Technologies) used to administer the vector (52, 53). A 20-gauge spinal needle was placed on the surface of the brain orthogonal to the skull to act as a guide for catheter insertion 2 cm into the pre-determined locations. Intravenous mannitol (typically 1.0 g/kg) was given as needed throughout the period of vector administration to minimize brain edema. In all treated children, the total vector volume of 1.8 ml was equally divided among 12 cortical locations delivered through 6 burr holes (2 locations at 2 depths through each burr hole), 3 burr holes per hemisphere. While the exact locations of the administration of the vector were subject specific, they were generally in the same regions of the brain, with the goal of providing safe, widespread distribution as has been previously described (53). Briefly, six trajectories were planned for each subject, with 3 bilateral paired trajectories targeting the subcortical white matter and entering through the middle of the superior frontal gyrus, immediately anterior to the precentral gyrus and the posterior superior parietal lobule. Deep targets for each hemisphere relative to the mid-commissural point (midpoint of the intercommissural line between the anterior and posterior commissures) was as follows:

Anterior frontal: X=25 mm lateral, Y=30 mm anterior, Z=25 mm superior

Posterior frontal: X= 20 mm lateral, Y=2 mm anterior, Z= 30 mm superior

Parietal: X=20 mm lateral, Y=35 mm posterior, Z=30 mm superior

Entry points were planned at the closest gyrus which was perpendicular to the planned target with the goal of the deep target being roughly 25 mm below the cortical surface. To create perpendicular tracts that would minimize the risk of an angular trajectory skewing into a sulcus, the deep target was adjusted up to 5 mm in any direction, also ensuring that the deep target was within the white matter below the bottoms of the adjacent sulci to facilitate wider spread of the vector solution, as described previously (53). Following administration of vector to the deep target at each of the six bilateral locations, catheters were withdrawn roughly 10 mm where a second infusion was completed at each site. An example of surgical planning for subject V1 is provided (fig. S2). The vector was administered at a rate of 2.0 $\mu\text{l}/\text{min}$ to each of the 6 sites (the deeper of the 2 sites through each burr hole) simultaneously by a microperfusion pump (Harvard Instrument PHD 2000 Infuse/Withdraw Multichannel Syringe Pump, Harvard Apparatus, Holliston, MA) driving 6 Hamilton syringes (Hamilton Syringe, Reno, NV). After the specified dose was administered, the catheters were left in place for 5 min to assure tissue penetration. The catheters were then withdrawn approximately half-way from the bottom of the catheter tract to the brain surface, and the remaining 50% of the dose was administered, in parallel, to each of the 6 additional sites as described above. For both cohorts 1 and 4, the average time for total vector infusion averaged 151.1 ± 1.0 min, surgery duration was 358 ± 43 min and time under anesthesia was 481 ± 55 min (see tables S2 and S3 for details). Following vector administration, the incision was closed with standard techniques. A post-operative CNS MRI was performed within the first 48 hr following the surgical procedure to assess for bleeding or other possible peri-operative adverse events.

The first 6 children in cohort 1 (V1 to V6) received a total dose of 9.0×10^{11} genome copies (gc) delivered in equal doses at each of 12 sites (7.5×10^{10} gc per site). In some children, foci of T2 hyperintensity localized to the sites of administration were observed in the day 1 post-

surgical T2 FLAIR, diffusion weighted imaging (DWI), and apparent diffusion coefficient (ADC) MRI. These abnormalities persisted in subsequent CNS MRIs (6 to 12 months post-administration) in most cases, while in others it resolved (see fig. 1 and fig. S3 for examples). The volume of hyperintensity was estimated on the T2-FLAIR MRI images by defining a region of interest (ROI) that outlined each area of increased signal intensity on all slices. The total number of voxels in the ROI was determined and multiplied by the volume of each voxel to produce a total volume (table S5). Although there were no clinical correlates attributable to the persistent localized foci of T2 hyperintensity, in agreement with the FDA, IRB and DSMB, the dose for subsequent children (V7, V8 in cohort 1 and S3, S4, S5 in cohort 4) was reduced to a total dose of 2.85×10^{11} gc (2.4×10^{10} gc per site). Comparisons within each time point, pre and post vector administration, between dose groups were made using the Fisher exact test in a 2 x 2 table (High-low dose vs. number of positive and negative abnormalities) for each parameter (T2, DWI and ADC).

Post-vector administration assessment

Each child was monitored post-operatively in the recovery room and pediatric intensive care unit, and once stable, transferred to an inpatient bed. The children were discharged from the hospital an average 3.0 ± 1.0 days post-surgery. All families were asked to remain in the proximity of the hospital until the day 14 evaluation.

Children in cohorts 1 and 4 were assessed at Weill Cornell at days 7 and 14, and at months 1, 6, 12, and 18 following treatment for safety parameters. At month 2 and 3, they were additionally assessed for adverse effects at the child's personal physician's office (see table S11 for timeline of safety assessments). For one subject (V6), who was unable to return to Weill Cornell for follow up visits, the study team went to the subject's home location to carry out some of the follow-up visits. All clinical efficacy evaluations for cohort 1 using the clinical rating scale

were videotaped for blinded assessment by 3 pediatric neurologists (4) (table S7). The family for subject V8 dropped out of the 18-month follow-up part of the study, citing difficulty in traveling with the child. At month 22 after therapy, we sent a team to assess the child. Because none of the assessments were within the mandated 18 month \pm 30 day study period (table S11), the data was not used for efficacy analysis.

Safety parameters

The safety parameters were assessed over the course of the 18 months for both cohorts 1 and 4 (table S11). Adverse event information was captured and the clinical monitor determined the attribution of adverse events to the study drug. Based on prior experience indicating possible localized inflammation and/or edema at the sites of administration when the vector concentration at the tip of the catheters are the highest, the CNS MRI pre- and post-administration (days 1, months 6, 12 and 18) were assessed for the presence of T2 FLAIR and diffusion abnormalities at the estimated sites of administration (fig. 1).

Anti-vector immunity

Serum AAVrh.10 neutralizing antibody titers from cohorts 1 and 4 over time were quantified by an in vitro assay with HEK293-ORF6 cells. An AAVrh.10 vector expressing a luciferase reporter transgene (AAVrh.10Luc) was incubated with 2-fold serial dilutions of sera at 37°C for 45 min and then used to infect cells at a multiplicity of infection of 3000 genome copies/cell. At 48 hr post-infection, luciferase activity was assessed with cell lysate using the Luciferase Assay System (Promega, Madison, WI). The neutralizing antibody titer was expressed as the reciprocal of serum dilution at which 50% inhibition of AAVrh.10Luc was observed (58). Similarly, CSF AAVrh.10 neutralizing antibody titers from cohort 1 over time (on pre and one post administration timepoint) were quantified by an in vitro assay with HEK293-ORF6 cells as described above for the serum samples.

For anti-capsid and anti-transgene cellular immunity, blood samples were collected from cohort 1 and cohort 4 at timepoints specified in the timeline (table S11), fractionated and sent to the Immunology Core, Gene Therapy Program at the University of Pennsylvania. Isolated peripheral blood mononuclear cells (PBMC) were assayed for T-cell responses to the AAVrh.10 capsid and CLN2 transgene by INF- γ ELISpot with 3 pools of AAVrh.10 capsid peptides and 2 pools of transgene peptides, each synthesized as libraries of 15-mers with a 10 amino acid overlap (Mimotopes). As a control, the potential for toxicity of these peptides was evaluated for the inhibition of a stimulated response in a standard blood mononuclear cell preparation to a positive control peptide library, a panel of MHC class 1 restricted viral peptides from cytomegalovirus, Epstein-Barr virus and influenza virus (59). Stimulation with phytohemagglutinin (PHA) provided the positive assay control; the negative control was growth media. The number of spot-forming units (sfu) per 10^6 PMBC was counted. Data accepted as valid included only samples that had positive PHA response and low sfu for the media stimulated control.

Relative quantity of CSF TPP1

Human TPP1 protein expression was assessed in cerebral spinal fluid (CSF) collected at pre- and one post-administration follow-up visit, (the Weill Cornell IRB restricted post-therapy CSF assessment to 1 time-point). CSF from 3 healthy children were mixed in equal volume and 1-10 μ l were analyzed to serve as positive control. CSF from the study children both pre- and post-vector administration (10 μ l) was analyzed in a 4 to 12 % SDS-polyacrylamide gel and transferred onto a polyvinylidene difluoride membrane. The membrane was treated with rabbit anti-human TPP1 antibody, 1:1000 diluted in 5 % dry milk in PBS, (Abcam) for 1 hr, 23°C and then washed 4 times with PBS plus 0.05 % Tween-20 (PBS-Tween). The membrane was then incubated with 1:5,000 diluted horseradish peroxidase (HRP)-conjugated goat anti-rabbit IgG

(Abcam) for 1 hr, 23°C, washed 5 times with PBS-Tween and developed with Enhanced Chemiluminescence (ECL) Plus reagent (Thermo Scientific). The amount of TPP1 was quantified using Image J software and expressed as integrated band density in arbitrary units. Fold-increase (relative quantity) of TPP1 following vector administration was compared to the pre-administration amount of TPP-I for the same child. The % normal amount was determined by using the TPP-I band density in the linear range of normal levels normalized to 10 µl.

CNS MRI % grey matter

As controls for the MRI % grey matter assessment of the treated children, 62 MRI datasets were acquired from 47 untreated CLN2 patients. The control data included 12 untreated controls (cohort 2), the pre-therapy time points for the n=8 children in cohort 1 and n=5 in cohort 4 (the "screening" and "pre-therapy" assessments; table S11) and n=24 children in the screening study that did not participate in the study. For the treated children in cohort 1, there were 3 post-therapy MRI evaluations, at 6, 12 and 18 months.

All imaging data were acquired on a 3.0 Tesla GE MRI scanner with an 8-channel head coil. A sagittal BRAVO sequence was used with isotropic (1.0 x 1.0 x 1.0 mm) resolution as previously described (36). Percent gray matter (%GM; % of total brain volume) was calculated using the FAST segmentation program within the FSL Software Library (FMRIB, Oxford UK) (60).

The skull was digitally removed prior to segmentation using the FSL brain extraction tool (61). The %GM was determined by multiplying the mean value of the tissue probability by the tissue volume and dividing by the total of gray matter + white matter (WM) + CSF (62). A sigmoidal function was tested for the imaging variables of the untreated children as defined by:

$$\%GM = \frac{A_1}{1 + e^{A_2(Age - A_3)}} + A_4$$

where A_1 is the amplitude of the sigmoidal curve, A_2 determines the sharpness of the rate of decline, A_3 is the time shift and A_4 is the decay asymptote. Since the age of onset of CLN2 is variable, and thus age is not an independent variable, the data was fitted using a total least squares method. Unlike conventional least squares regression models, total least squares regression is not scale invariant, and so requires a scaling rule to be specified. Based upon inspection of the %GM dataset, we chose $\%GM_{\text{scaled}} = 27.05 * \%GM - 4.66$, such that the numerical range of $\%GM_{\text{scaled}}$ approximated the range of subject ages in years in order to make the dynamic range of the x and y axis roughly equivalent. After fitting the natural history cohort using this method, the scaling factor was removed.

Fitting was performed using a bootstrap technique. For each bootstrap, the 62 points from the CLN2 natural history dataset were resampled with replacement, i.e. duplicates were allowed, using MATLAB 2019a (Mathworks). This process was repeated 1000 times. Next, the results from each run of the bootstrap were fitted with the sigmoid of Equation 1, consisting of 100 points across an age range of 2 to 12 yr. After completion of 1000 runs, the $\%GM_{\text{scaled}}$ mean value and 95% confidence intervals were calculated for each of the 100 points. The resulting functions were closely approximated by sigmoids as expected.

In order to eliminate the time variable from the analysis, the rate of change of %GM was plotted *vs* %GM, allowing for direct comparison of subjects with different ages of disease onset. If the %GM varies with age according to the sigmoid of equation 1, then the %GM/yr *vs* %GM is a parabolic function. Since the parabola was calculated by first taking the time derivative of the sigmoid, and therefore each data point represents the difference of the neighboring data-points of the %GM sigmoid, the error in the parabolic function at each value of %GM was estimated simply from the quadrature sum of errors in the sigmoid as:

$$\delta\%GM/\text{yr}(t) = \text{sqrt} (\delta\%GM(t)^2 + \delta\%GM(t-1)^2)$$

where $\delta\%GM(t)$ is the difference between the sigmoidal function and its 95% confidence interval at time t .

Assessment of the effect of therapy *vs* the untreated controls was determined by comparing the difference between the 95% confidence intervals of the slopes of %GM decline in treated children in cohort 1 and the 95% confidence interval of the sigmoidal fit to CLN2 MRI natural history data at a given disease severity defined by the %GM. This method accounts for both ceiling and floor effects as estimated by the upper and lower asymptotes of the 95% confidence intervals of the sigmoids. Mean values of treated children above the 95% confidence interval was considered an improvement compared to the untreated controls. This data was further used to compare the MRI % grey matter change/yr with the range of change/yr for the untreated children with matching % grey matter.

Vision-related parameters

Given the severity of motor and cognitive abnormalities associated with CLN2 disease, all children were examined while under sedation. The baseline ophthalmic evaluation included complete anterior segment and dilated exam, fundus photography (RetCam, Clarity Medical Systems Inc), spectral domain optical coherence tomography (OCT, Heidelberg Engineering), fluorescein angiography (FA, Heidelberg Engineering and RetCam) and indocyanine green angiography (ICGA, Heidelberg Engineering). The ocular exam, OCT, FA, and ICGA were used to establish the extent of retinal degeneration in each patient based on the Weill Cornell Batten Scale as previously described (39). In addition to the baseline exam, 5 children underwent ophthalmic evaluation, with anterior segment and dilated exam and fundus photography, following gene therapy administration. In one of these children, OCT evaluation was also performed after therapy. In those children with OCTs, for each eye on each examination date, central subfield thickness (CST) was calculated by Heidelberg software as previously described

(38). In the 5 children with follow-up evaluation, the clinical exam and fundus photography were used as a qualitative assessment of retinal disease progression. Quantitative assessment of the progression of CLN2-related retinal degeneration in the one child with follow-up OCT was determined and compared to the natural history graph derived using CST as previously described (38).

Clinical neurologic rating scale

There are 2 clinical neurologic rating scales for CLN2 disease: the original Hamburg scale described by Steinfeld et al (63); and the Weill Cornell scale described by Worgall et al (4). Details of the 2 scales are described in table S1. The 2 scales are identical in 2 parameters: the “Motor” and “Language” parameters in the Hamburg scale are the same as the “Gait” and “Language” parameters in the Weill Cornell Scale. Each of these scales had additional parameters which were not used in assessment of the efficacy of the therapy because of variability, dependency on care giver parameters, or irrelevance to CNS disease. The “Motor” and “Language” (Hamburg scale) and the identical “Gait” and “Language” (Weill Cornell scale) were used to quantify the rate of clinical decline of the treated and untreated children. Since the “Gait” (Weill Cornell) and “Motor” (Hamburg) parameters are identical (table S1), to avoid confusion, we used the term “Motor” instead of “Gait” used in the Weill Cornell scale. As a comprehensive clinical neurologic assessment, the “motor” and “language” scores (each scale 0-3) were summed to generate a “CLN2 disease neurologic rating scale” (64). These were the identical parameters used in the multi-institutional collaborative CLN2 disease “natural history” publication (5), and the parameters for the FDA approval of cerliponase alfa (31).

For cohorts 1 and 2, the clinical assessment of motor + language was performed prospectively using defined standard operating procedures (SOPs) based on 3 to 4 observers, with specific rules on how the data was evaluated. The primary, on-site assessor was a pediatric

neurologist who had been trained on implementing the scale. The assessment of each child was videotaped by a trained technician following a SOP for recording the assessment and editing for review by 2 to 3 other pediatric neurologists who were trained on implementing the scale. The neurologists that assessed the video recording were blinded to the subjects' treatment status. In the event of discrepancy of more than 1 point between the 2 blinded scorers, a 3rd pediatric neurologist, also blinded, scored the video in order to act as a tie-breaker. The final score was an average of the assessment of the 3 to 4 reviewers (primary + 2 to 3 additional reviewers) to minimize bias and subjective interpretation. The variance among the observers was not significant (table S7). As a further validation of the methods used to assess the robustness of the quantitative neurologic assessment, reproducibility of the motor and language scale was validated by comparing repeat assessments of the severity of CLN2 disease in the same child carried out within <1.5 months, a time when deterioration would not be detectable. The mean assessment of the 3 to 4 observers was identical over this short time interval (table S5).

Individuals other than the principal and co-principal investigators collected, tabulated and verified the clinical parameters and adverse effects. To quantify the annual rate of decline of motor and language, linear regression of the consensus motor + language score over time was taken for each subject in the treatment (cohort 1) and untreated cohort (cohort 2). As the age of each subject was in days, the slope obtained was multiplied by 365 days to provide an annual rate of decline for each subject and the individual rates were then averaged to provide the annualized rate of decline \pm standard deviation for the cohort. The individual data points for all subjects in cohorts 1 and 2 are in Table 2 and table S11.

Additional Safety Data

In addition to the treated cohort (cohort 1), there were 5 children (cohort 4) assessed in the screening protocol that did not fulfill the inclusion/exclusion criteria for the treated vs

untreated trial because of disease severity and/or genotype. At the request of the families, these children were enrolled in a secondary safety study, under a different protocol where they received the same therapeutic intervention but for the purpose only of adding to the safety profile of AAVrh.10hCLN2 (NCT01161576, see table S10 for Inclusion/Exclusion criteria, Table 1 for demographics and table S11 for timeline of assessments).

Secondary Parameters

The parents of all treated and untreated children were asked to complete the CHQ or ITQoL (depending on age) quality of life questionnaires and the children were also assessed with the Mullen scale (65-68). The Infant Toddler Quality of Life Questionnaire Parent Form (ITQoL-PF97) was used to assess parents of 2 months to 5 year-old subjects while the Child Health Questionnaire Parent Form (CHQ-PF50) was used to assess parents of 5 to 18 year-old subjects (table S12). These quality of life questionnaires were completed by at least one parent/legal guardian at the times of assessment. The survey was administered independently to each parent to minimize observer bias if both parents were present. The Mullen pediatric developmental psychological rating scale, was administered by either a neuropsychologist or trained study coordinator. This scale assesses gross motor, cognitive, receptive and expressive language, adaptive behavior and fine motor skills.

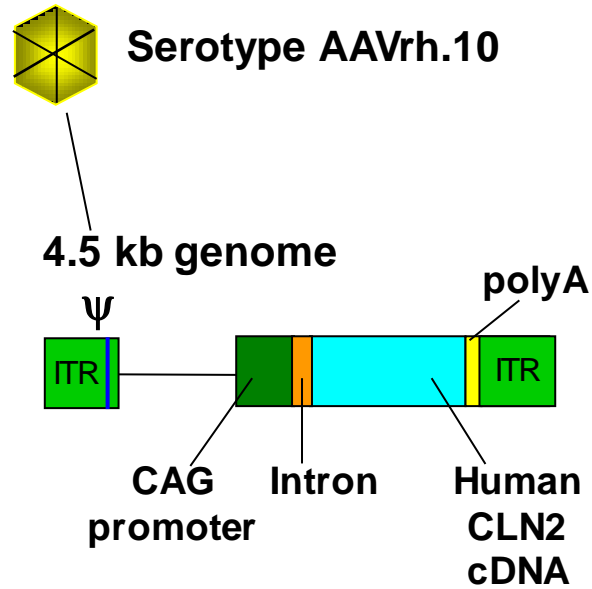


Fig. S1. AAVrh.10hCLN2 vector. The vector is comprised of an AAVrh.10 capsid encompassing a genome composed of 5' and 3' AAV2 inverted terminal repeats surrounding an expression cassette including: the enhancer from human cytomegalovirus, promoter, splice donor and left hand intron sequence from chicken β -actin /right hand intron sequence and splice acceptor from rabbit β -globin, the normal human CLN2 cDNA, and rabbit β -globin polyA.

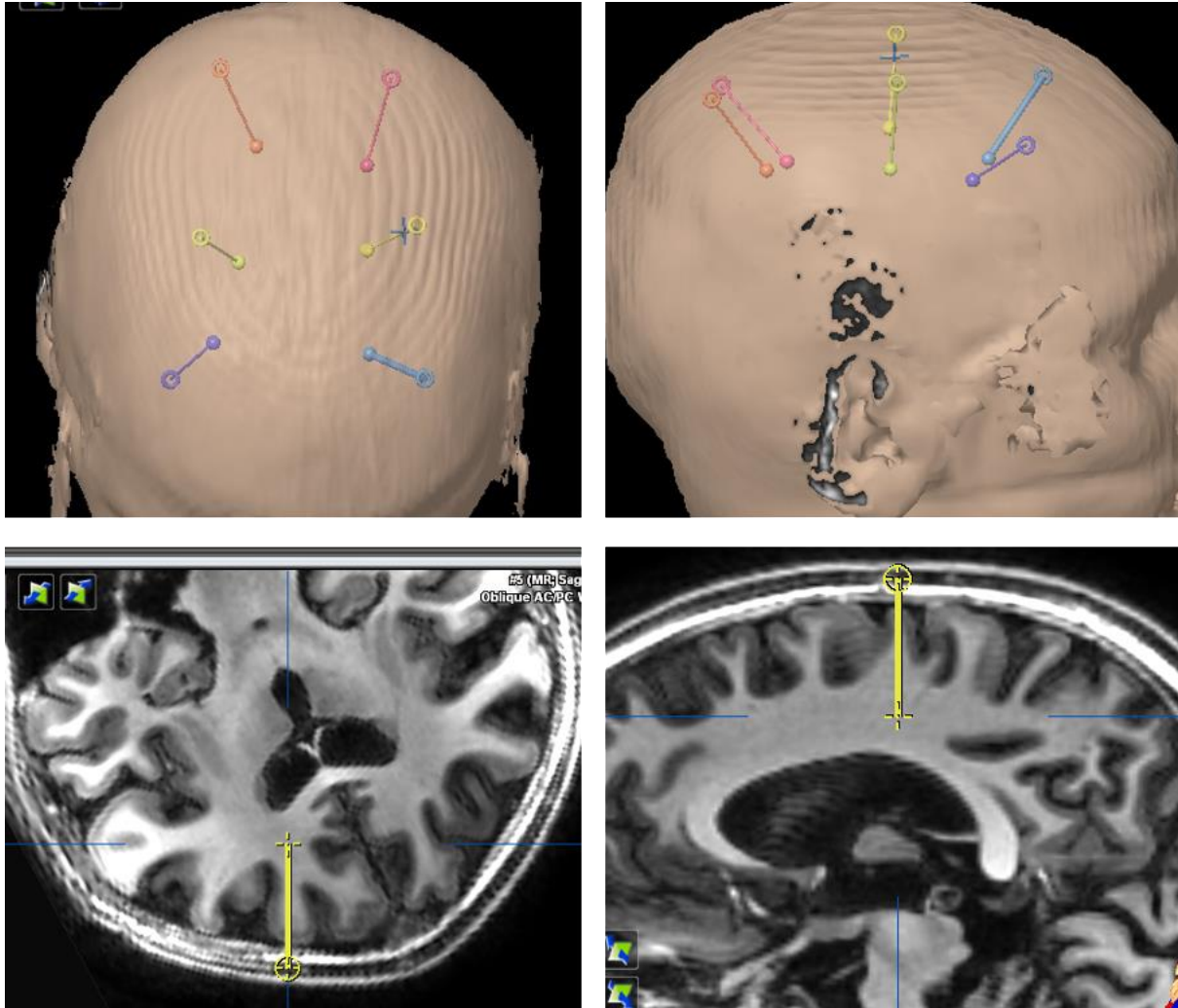
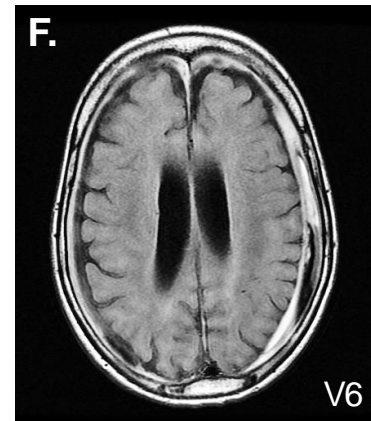
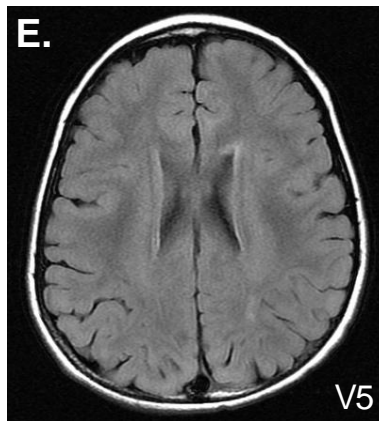
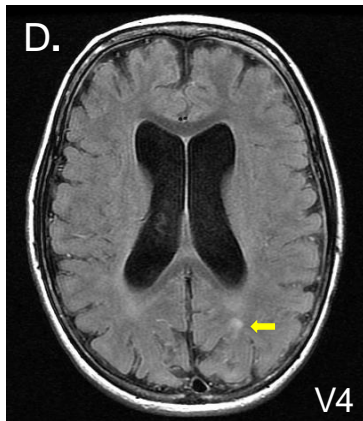
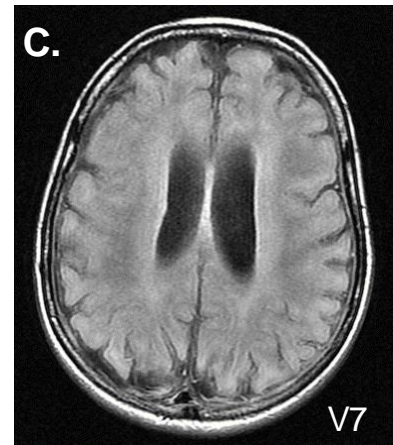
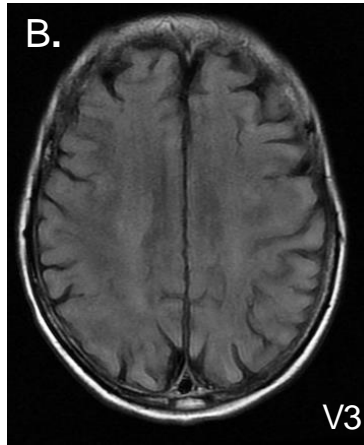
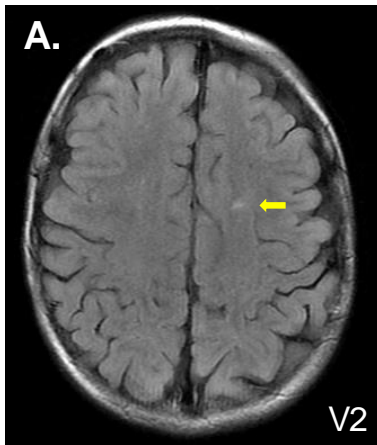


Fig. S2. Trajectory planning for gene therapy infusions. Example of trajectory planning for a study subject showing six planned trajectories (bilateral anterior frontal, posterior frontal and parietal) overlaid on the reconstructed subject head in a frontal (upper left) and sagittal (upper right) views. An example of a single trajectory (left posterior frontal) from surface to the deep target shown through the long axis of the trajectory in oblique coronal (lower left) and sagittal (lower right) views.

T2 FLAIR 6 month

T2 FLAIR 6 month

T2 FLAIR 6 month



T2 FLAIR 12 month

T2 FLAIR 12 month

T2 FLAIR 12 month

Fig. S3. Axial T2 FLAIR (T2 FLAIR) assessment of participants after therapy. Additional images of post-treatment examples of Axial T2 FLAIR (T2 FLAIR) MRI assessment of subjects where the T2 hyperintensities observed were minimal or absent. **A.** Participant V2, 6 month post-administration, minimal T2 hyperintensity observed; **B.** V3, 6 months, no T2 hyperintensity observed; **C.** V7, 6 months, no T2 hyperintensity observed; **D.** V4, 12 months, minimal T2 hyperintensity observed. **E.** V5, 12 months, no T2 hyperintensity observed. **F.** V6, 12 months, no T2 hyperintensity observed. Yellow arrows identify any abnormalities at the site of vector administration.

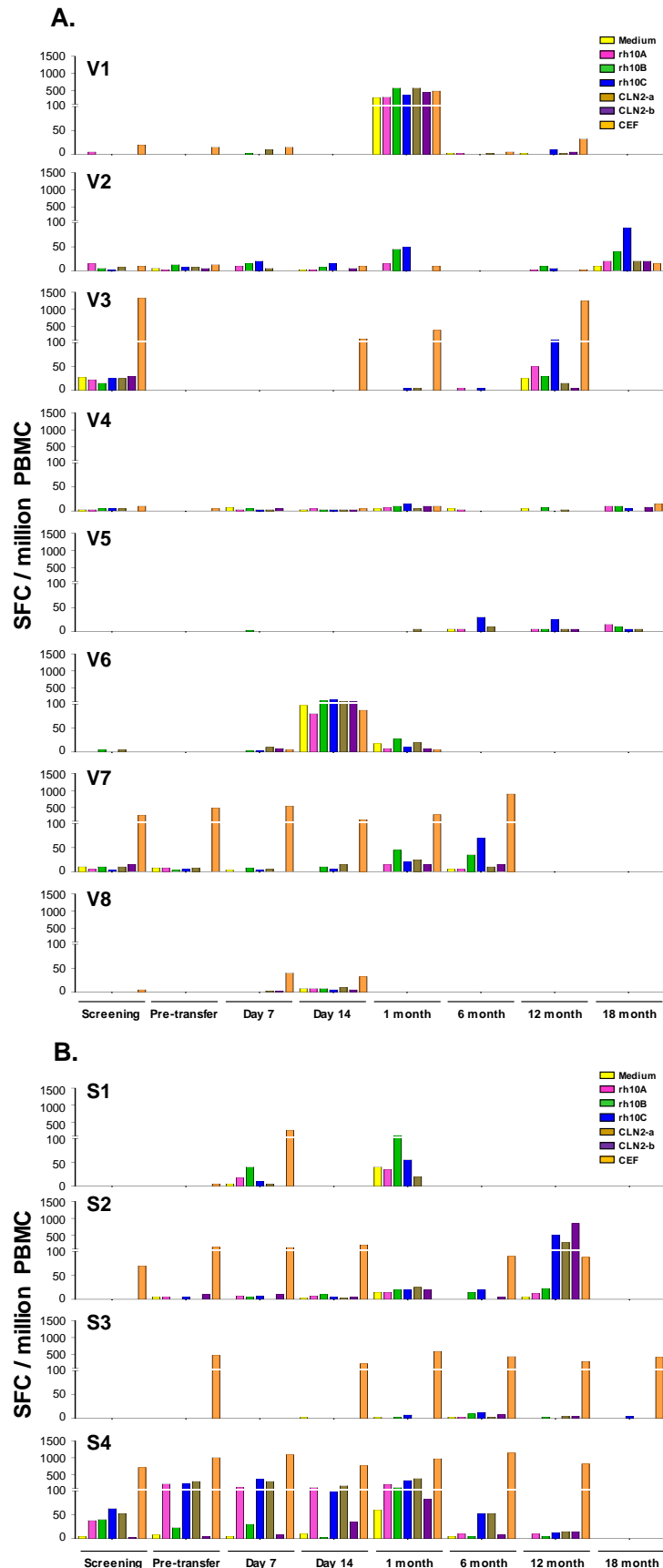


Fig. S4. T cell responses to AAVrh.10 capsid and CLN2 transgene. Evaluated by IFN- γ ELISPOT of peripheral blood mononuclear cells (PBMC) stimulated with AAVrh.10 capsid peptides or CLN2 transgene peptides. Stimulation with phytohemagglutinin (PHA) provided the positive assay control; the negative control was growth media. A panel of MHC class 1 restricted viral peptides from cytomegalovirus, Epstein-Barr virus and influenza viruses (CEF) served as a positive control peptide library reference. Data is plotted as spot-forming units per million PBMC. PBMC were derived from sera obtained at 1 or 2 times before (screening and pre-transfer) and at days 7, 14 and months 1, 6, 12 and 18 after vector administration and stimulated with each of 3 pools (A, B, and C) of AAVrh.10 capsid peptides or with each of 2 pools (A and B) of CLN2 transgene peptides or a positive control peptide pool (CEF). Peptide pools were 15-mers overlapping by 10. **A.** Participants in cohort 1. V7 received the lower dose (2.85×10^{11} gc). **B.** Participants in Cohort 4 (samples were not available for S5). SFU = spot forming units. S2 and S3 received the lower dose (2.85×10^{11} gc). In samples from some subjects there was no response to the positive control likely due to these children not having prior exposure to these infectious agents.

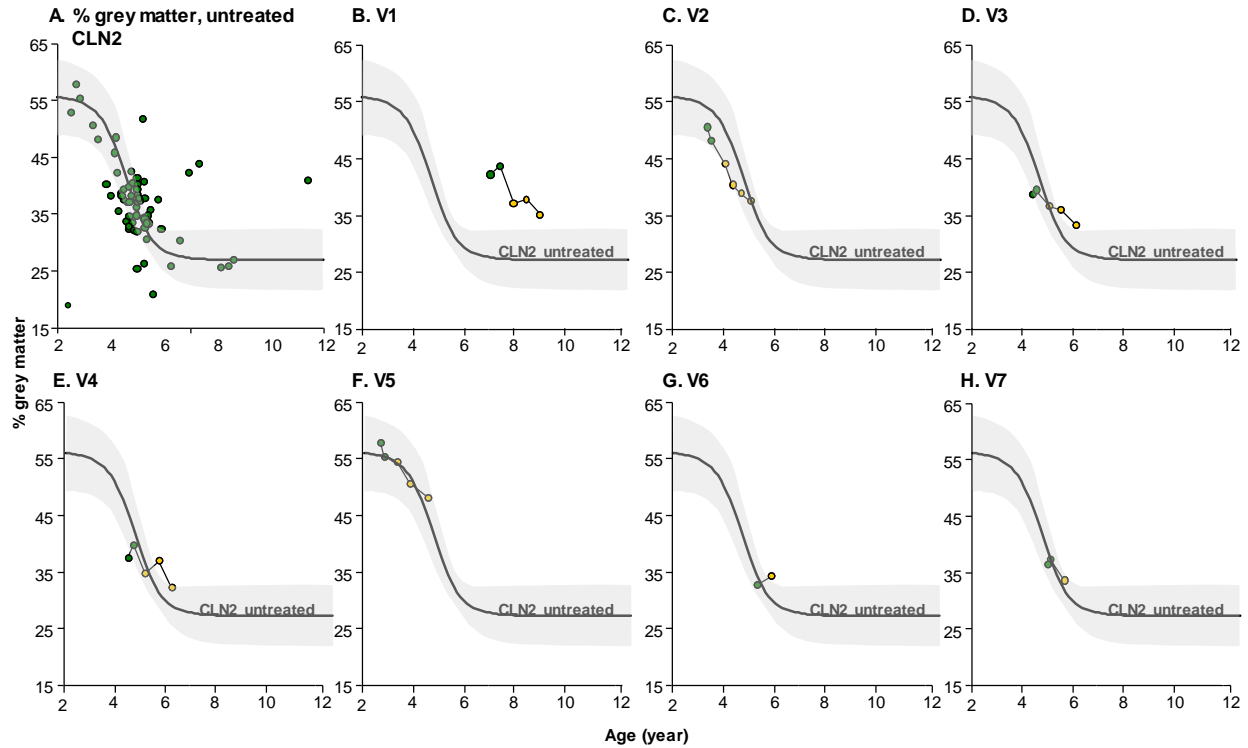


Fig. S5. MRI assessment of the treated CLN2 children versus untreated CLN2 children. **A.** Percent (%) grey matter vs age for untreated CLN2 children (n=62 MRI scans from 47 participants, green dots). The solid grey line represents the mean of 1000 bootstrap sigmoidal fits to the CLN2 natural history data. The grey shaded area represents the 95% confidence intervals of those fits. **B-H.** Cohort 1 participants V1 (B), V2 (C), V3 (D), V4 (E), V5 (F), V6 (G), and V7 (H). V7 (panel H) received the lower dose (2.85×10^{11} gc). MRI performed on each cohort 1 participant at time-points pre (green dots) and post (tan dots) vector administration overlaid on grey shaded area representing the % grey matter values vs age of sigmoidal and linear fits to CLN2 natural history subjects from panel A.

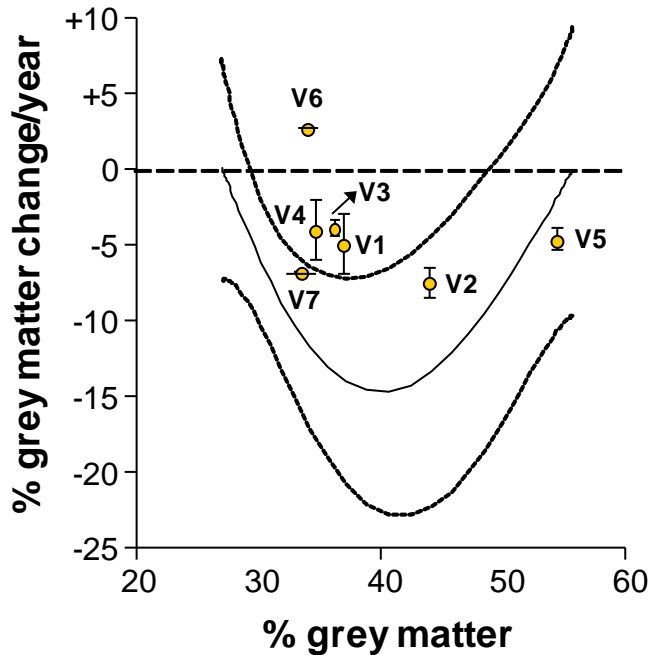
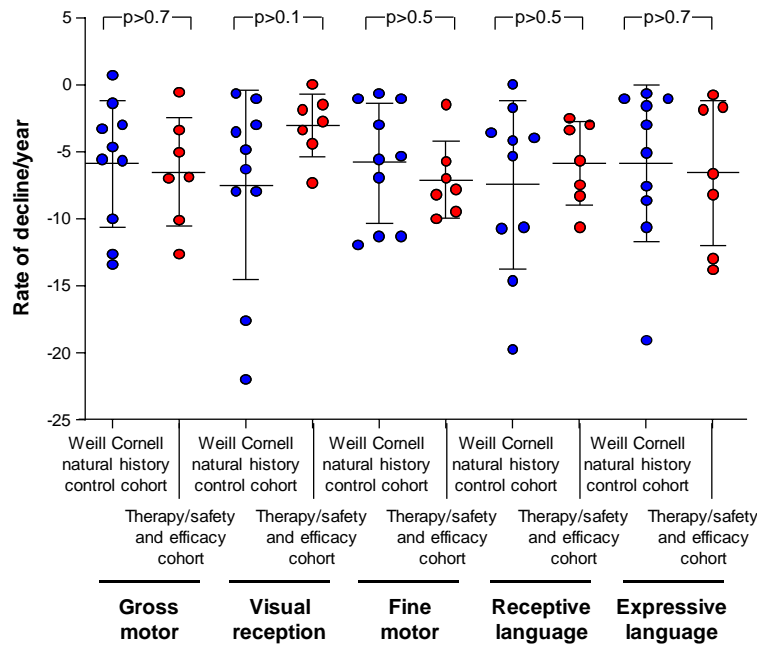


Fig. S6. Quantitative MRI assessment of the treated CLN2 children (cohort 1) versus untreated CLN2 children. Shown is the MRI % grey matter decline per year vs % grey matter, as assessed by MRI. In untreated children after birth, the decline in grey matter starts slowly with near zero slope, then declines rapidly and then slows again, appearing as a sigmoid curve. A plot of the rate of decline vs % grey matter is therefore a parabola with respect to either time or % grey matter. The dashed line parabolas represent the upper and lower 95% confidence intervals of the % rate of grey matter decline for the natural history cohort (fig S5A). The solid line parabola represents the average change of % grey matter change/year as a function of the % grey matter for the untreated children. Data points from treated subjects with error bars lying above the upper dashed line had a slower rate of decline of % grey matter compared to untreated controls. Subject V5 was the youngest trial participant and thus was at the early stage slow rate of decline and the effect of therapy was not yet apparent. One subject (V6) for whom there was a slower rate of decline only had one post treatment scan and error bars could not be calculated. See fig. S5 for the data from which the % grey matter decline/yr of the treated and untreated children were determined. Subject V7 received the lower dose (2.85×10^{11} gc).

A. Individual scores



B. Mullen score sums

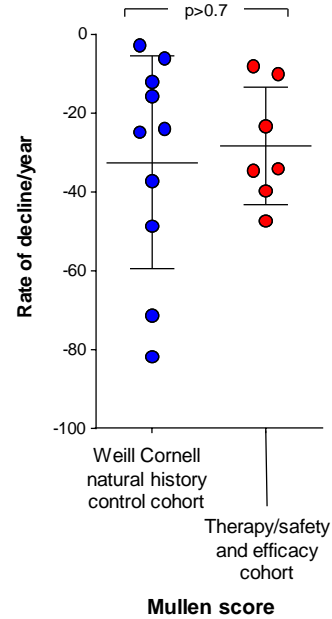


Fig. S7. Mullen scale quantitation of the rate of decline for cohorts 1 (red, treated) and 2 (blue, control). **A.** Linear regression assessed for the scores of each subject in gross motor, visual reception, fine motor, receptive language, and expressive language domains over time to calculate their individual rate of decline within each cohort. **B.** Individual rates of decline for all participants within a cohort were then averaged to calculate the rate of decline/year for the combination of domains or the total Mullen score for each individual cohort. The rates of decline/year for each cohort are plotted as a mean rate of decline with the error bars representing plus and minus one standard deviation from the cohort mean, and the individual rates of declines for each subject are overlaid on the mean data. The p value was calculated using a two-tailed unpaired Student t-test (GraphPad v8.0).

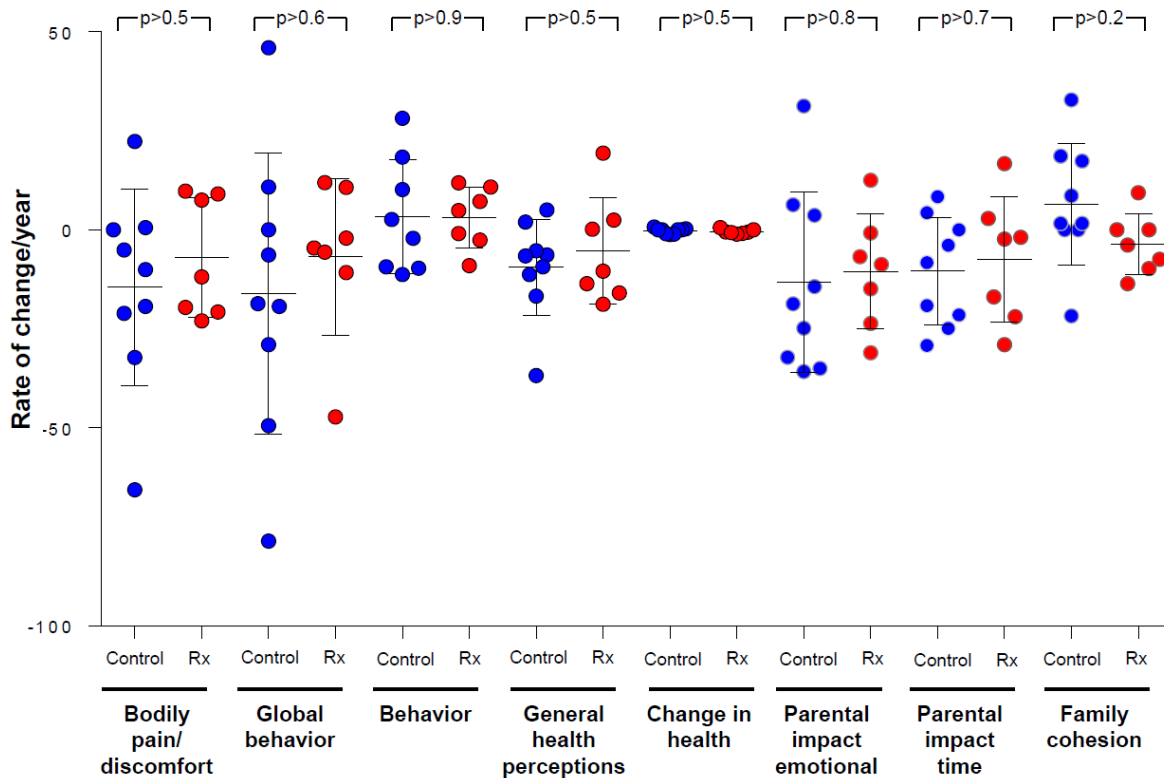


Fig. S8. Impact of treatment on quality of life as assessed by age-dependent quality of life questionnaires. The parents of all cohort 1 and cohort 2 children were asked to complete either the CHQ or ITQoL (depending on age) quality of life questionnaires. The Infant Toddler Quality of Life Questionnaire Parent Form (ITQoL-PF97, assessing 13 different parameters) was used to evaluate parents of 2 months to 5 year-old participants while the Child Health Questionnaire Parent Form (CHQ-PF50, assessing 14 different parameters) was used to evaluate parents of 5 to 18 year-old participants. During the course of the study as the child aged, they may have aged out of ITQoL and been assessed by CHQ. In order to determine if there was any impact of treatment on the quality of life as determined by these questionnaires, we focused on the 8 parameters that were identical in the two questionnaires. Linear regression assessed for each subjects' scores in each of 8 parameters (bodily pain/discomfort, global behavior, behavior, general health perceptions, change in health, parental impact emotional, parental impact time, family cohesion) over time to calculate their individual rate of decline within each cohort. The rates of decline/year for each cohort are plotted as a mean rate of decline with the error bars representing plus and minus one standard deviation from the mean, and the individual rates of declines for each subject are overlaid on the mean data. The p value was calculated using a two-tailed unpaired Student t-test (GraphPad v8.0). Rx – treated cohort.

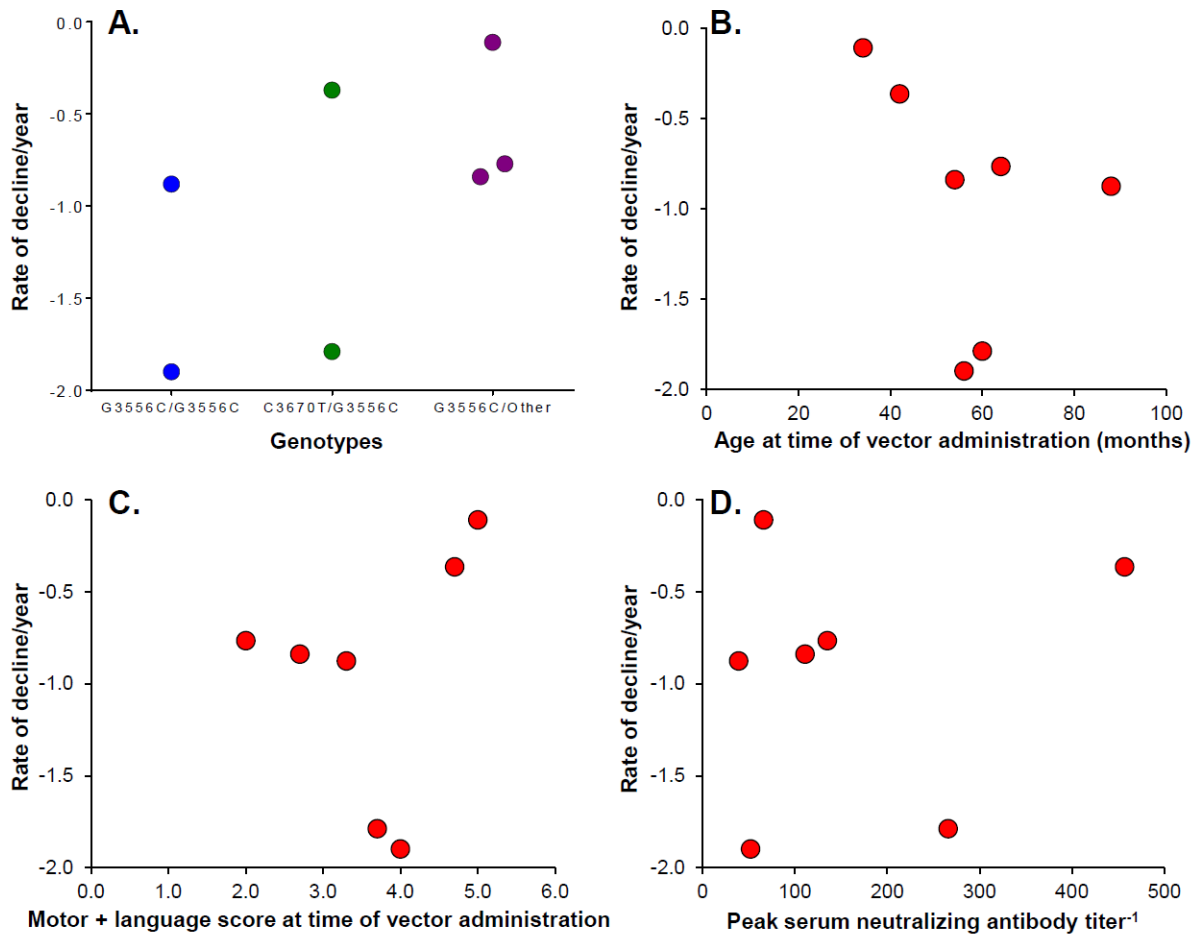


Fig. S9. Correlation of various parameters to the rate of decline of motor + language of cohort 1. **A.** Impact of genotype on the rate of decline. Rate of decline for each participant was plotted with respect to genotype: homozygous G3556C/G3556C (blue), heterozygous C3670T/G3556C (green) or heterozygous G3556C/Other genotypes (purple). **B.** Rate of decline as a function of age at time of vector administration. The rates of decline/year for each participant was plotted as a function of age at treatment (in months) for the treated cohort. **C.** Rate of decline as a function of the motor + language score at time of vector administration. The rate of decline/year for each participant was plotted as a function of the combined motor + language scores (scale of 0 to 6) the treated cohort at the time of treatment. **D.** Impact of the peak neutralizing antibody response on the rate of decline. Serum anti-AAVrh.10hCLN2 neutralizing antibody titers were determined at multiple time points through the trial for participants in cohort 1. The rates of decline/year for each subject are plotted against their peak antibody titer.

Table S1. CLN2 disease severity clinical rating scales.¹

¹ The shaded area identifies the neurologic parameters used to assess clinical efficacy. The gait and language subscales in the Weill Cornell scale are equivalent to the motor and language subscales in the Hamburg scale (shaded in grey); to avoid confusion, we refer to “gait” in the Weill Cornell scale as “motor” as per the combined published natural history data (5).

² Steinfeld, R, et al, American Journal of Medical Genetics 2002; 112: 347-354 (63).

³ Worgall, S, et al, Neurology 2007; 69:521-3(4).

		Hamburg scale²			Weill Cornell scale³
Motor	3	Normal	Gait	3	Normal
	2	Falls, obvious clumsiness		2	Abnormal, but independent
	1	No unaided walking		1	Abnormal, requires assistance
	0	Immobile		0	Non-ambulatory
Language	3	Normal	Language	3	Normal
	2	Abnormal		2	Abnormal
	1	Barely understandable		1	Barely understandable
	0	Unintelligible or no speech		0	Unintelligible or no speech
Visual function	3	Recognizes desirable objects, grabs	Motor	3	None of below
	2	Grabbing for objects uncoordinated		2	1 of below
	1	Reacts to light		1	2 of below
	0	No reaction to visual stimuli		0	Myoclonus and chorea / tremor / athetosis and upgoing toes
Seizures	3	None in 3 months	Feeding	3	No dysfunction
	2	1-2 seizures per month		2	Mild
	1	1 per month		1	Moderate
	0	>1 per month		0	Gastrostomy tube dependent

Table S2. Vector infusion time and operating room surgery and anesthesia duration in cohort 1 participants.

¹ In all children, the total vector volume of 1.8 ml was equally divided among 12 cortical locations delivered through 6 burr holes. There were 2, 150 μ l infusions through each burr hole (2 locations at 2 depths through each burr hole), 3 burr holes per hemisphere. The rate of infusion was 2 μ l/min. There were slight variations on time based on pump calibration. After the specified dose was administered over a period of ~ 75 min to the 6 sites, the catheters were left in place for 5 min to assure tissue penetration. The catheters were then withdrawn approximately half-way from the bottom of the catheter tract to the brain surface, and the remaining 50% of the dose was administered, in parallel, to each of the 6 sites (the less deep of the 2 sites through the burr hole).

² Surgery duration included time from when the surgeon started drilling the burr holes and pre-determined location, to when the last burr hole was sutured.

³ Duration under anesthesia is a surrogate for the entire time the child was in the operating room.

Patient identifier	Infusion 1 duration¹ (min)	Infusion 2 duration¹ (min)	Total infusion time (min)	Surgery duration² (min)	Under anesthesia³ (min)
V1	76	76	152	362	509
V2	77	75	152	360	472
V3	75	75	150	321	456
V4	75	78	153	355	473
V5	76	75	151	312	411
V6	75	75	150	344	476
V7	77	75	152	380	524
V8	76	75	151	369	494
Average \pm SD	75.9 \pm 0.8	75.5 \pm 1.1	151.4 \pm 1.0	350.4 \pm 23.5	476.9 \pm 34.6

Table S3. Vector infusion time and operating room surgery and anesthesia duration in cohort 4 participants.

- ¹ In subject S2-S5, the total vector volume of 1.8 ml was equally divided among 12 cortical locations delivered through 6 burr holes. There were 2, 150 μ l infusions through each burr hole (2 locations at 2 depths through each burr hole), 3 burr holes per hemisphere. The rate of infusion was 2 μ l/min. There were slight variations on time based on pump calibration. After the specified dose was administered over a period of ~ 75 min to the 6 sites, the catheters were left in place for 5 min to assure tissue penetration. The catheters were then withdrawn approximately half-way from the bottom of the catheter tract to the brain surface, and the remaining 50% of the dose was administered, in parallel, to each of the 6 sites (the less deep of the 2 sites through the burr hole).
- ² Surgery duration included time from when the surgeon started drilling the burr holes and pre-determined location, to when the last burr hole was sutured.
- ³ Duration under anesthesia is a surrogate for the entire time the child was in the operating room.
- ⁴ In subject S1 only, all 12 administrations were carried out in parallel, through 12 catheters. Each burr hole received administration through 2 catheters that were attached together and delivered at different depths.
- ⁵ The average total infusion time was calculated using the data for subjects S2 – S5; S1 was not included in the calculation, see footnote 4.

Patient identifier	Infusion 1 duration¹ (min)	Infusion 2 duration¹ (min)	Total infusion time (min)⁵	Surgery duration² (min)	Under anesthesia³ (min)
S1 ⁴	77	--	77	342	432
S2	76	76	152	482	630
S3	75	75	150	317	417
S4	75	75	150	362	492
S5	75	75	150	348	468
Average \pm SD	75.6 \pm 0.9	75.3 \pm 0.5	150.6 \pm 0.8	370.2 \pm 64.6	487.8 \pm 84.8

Table S4. CSF nucleated cells.¹

¹ Cerebral spinal fluid nucleated cell count

² Time after vector administration (months)

³ V7 received the lower dose (2.85×10^{11} gc).

Cohort 1			Cohort 4		
Subject	Month²	Cells/μl	Subject	Month²	Cells/μl
V1	18	0	S2	6	1
V2	12	2		12	0
V3	12	0	S3	6	0
V4	12	0		12	1
V5	12	0		18	1
V7 ³	6	1	S4	6	1
				12	2
				18	0

Table S5. Percent volume of the brain with MRI T2 hyperintensity.

¹ No T2 FLAIR was observed and hence volume is listed as 0.0%

² nd = scan not done

³ V7 received a lower dose than V1-V6; see Methods

	Time post-vector administration			
	24 hr	6 month	12 month	18 month
	Volume (%)	Volume (%)	Volume (%)	Volume(%)
V1	0.30	0.24	0.47	0.47
V2	0.00 ¹	0.06	0.23	0.20
V3	0.28	0.07	0.15	0.15
V4	0.12	0.11	0.32	0.28
V5	0.21	0.12	0.11	0.06
V6	0.07	0.00 ¹	nd ²	nd ²
V7³	0.11	0.08	nd ²	nd ²
Average	0.16	0.10	0.26	0.23
Standard deviation	0.11	0.07	0.14	0.16

Table S6. Quality of life questionnaires.^{1, 2, 3, 4}

- ¹ The parents of all cohort 1 and cohort 2 children were asked to complete either the CHQ or ITQoL (depending on age) quality of life questionnaires. For each visit, the ✓ indicates the quality of life questionnaire that was completed, and the other is left blank. If for a given visit neither quality of life questionnaire was completed, it states ND (not determined). The Infant Toddler Quality of Life Questionnaire Parent Form (ITQoL-PF97) was used to assess parents of 2 months to 5 year-old subjects while the Child Health Questionnaire Parent Form (CHQ-PF50) was used to assess parents of 5 to 18 year-old subjects
- ² The quality of life questionnaires were completed by at least one parent/legal guardian at the times of assessment. The survey was administered independently to each parent to minimize observer bias if both parents were present
- ³ During the course of the study as the child ages, they may age out of ITQoL, and be assessed by CHQ
- ⁴ Not done
- ⁵ This questionnaire was completed at the time of screening (visit 1) and also at the last visit (visit 2, which was typically ≥ 18 months from the screening visit

Subjects	First study visit 1 ⁵		Last study visit ⁵	
	ITQoL	CHQ	ITQoL	CHQ
Cohort 1				
V1		✓		✓
V2	✓			✓
V3	✓			✓
V4	✓			✓
V5	✓		✓	
V6		✓		✓
V7	✓			✓
V8	✓		ND	ND
Cohort 2				
C1	ND	ND	ND	ND
C2	✓			✓
C3		✓		ND
C4	✓		ND	ND
C5	✓		✓	
C6	✓			✓
C7	✓			✓
C8		✓		✓
C9	✓			✓
C10	✓			✓
C11		✓		✓
C12	✓			✓

Table S7. Coefficient of variation among observers in the CLN2 disease motor + language neurologic rating scale.

¹ To assess the variance in the measurements of the motor and language domains, we took the data obtained during the screening visit for all subjects

² Observer #1 is the “live” observer (pediatric neurologist) who performed the exam for the CLN2 disease neurologic rating scale; observers #2-4 were blinded to any patient or treatment related information and rated the children based on a videotape of the live assessment.

³ The coefficient of variation (CV; the standard deviation divided by the mean). The CV was calculated for each subject relative to the 4 reviewers to compare the scatter of variables involved in the testing. The average CV is reported for each parameter ± standard deviation of the group

Subject	Motor at Screening ¹							Language at Screening ¹							
	Observer ²				Mean	SD	CV ³	Observer ²				Mean	SD	CV ³	
	#1	#2	#3	#4				#1	#2	#3	#4				
V1	1	1	1	1	1.00	0.00	0.00	2	1	2	2	1.75	0.50	0.29	
V2	3	2	3	3	2.75	0.50	0.18	2	2	2	2	2.00	0.00	0.00	
V3	1	1	1	1	1.00	0.00	0.00	1	1	1	1	1.00	0.00	0.00	
V4	2	2	2	2	2.00	0.00	0.00	1	2	2	2	1.75	0.50	0.29	
V5	2	2	2	2	2.00	0.00	0.00	1	1	1	1	1.00	0.00	0.00	
V6	1	1	1	1	1.00	0.00	0.00	1	1	1	1	1.00	0.00	0.00	
V7	3	3	3	3	3.00	0.00	0.00	2	1	2	1	1.50	0.58	0.38	
V8	2	2	2	2	2.00	0.00	0.00	2	2	1	1	1.50	0.58	0.38	
C1	1	ND	ND	ND	-	-	-	1	ND	ND	ND	-	-	-	
C2	1	2	1	1	1.25	0.50	0.40	2	2	2	2	2.00	0.00	0.00	
C3	1	1	1	1	1.00	0.00	0.00	1	1	1	1	1.00	0.00	0.00	
C4	1	1	1	1	1.00	0.00	0.00	1	1	1	1	1.00	0.00	0.00	
C5	3	3	3	3	3.00	0.00	0.00	2	2	2	2	2.00	0.00	0.00	
C6	1	1	1	1	1.00	0.00	0.00	2	2	2	1	1.75	0.50	0.29	
C7	2	2	1	2	1.75	0.50	0.29	1	2	2	2	1.75	0.50	0.29	
C8	3	3	3	3	3.00	0.00	0.00	2	2	2	2	2.00	0.00	0.00	
C9	1	2	1	1	1.25	0.50	0.40	1	1	1	1	1.00	0.00	0.00	
C10	1	1	1	1	1.00	0.00	0.00	1	1	2	1	1.25	0.50	0.40	
C11	1	1	1	1	1.00	0.00	0.00	1	1	2	1	1.25	0.50	0.40	
C12	1	1	1	1	1.00	0.00	0.00	2	1	1	1	1.25	0.50	0.40	
Average CV							0.07±0.14	Average CV							0.16±0.18

Table S8. Reproducibility of motor and language assessment.¹

¹Data from n=5 study participants pre-therapy from either cohort 1 or 2, with 3 to 4 observers per data point. The data shown is for repeat assessment on the same child carried out within 42 days, a time when deterioration would not be detectable.

Tests	Motor (M)		Language (L)		Total (M+L)	
	Visit 1	Visit 2	Visit 1	Visit 2	Visit 1	Visit 2
V2	2.7	3.0	2.0	2.0	4.7	5.0
V3	1.0	1.0	1.0	1.7	2.0	2.7
V6	1.0	1.0	1.0	1.0	2.0	2.0
V7	2.0	2.0	1.7	1.7	3.7	3.7
C6	1.0	1.0	2.0	2.0	3.0	3.0

Table S9. Assessments of motor and language parameters for cohort 2.¹

¹ The motor + language data is provided for all subjects in cohort 2. The clinical assessment of motor + language was performed prospectively using defined standard operating procedures (SOPs) based on 3 to 4 observers, with specific rules on how the data was evaluated. The primary, on-site assessor was a pediatric neurologist who had been trained on implementing the scale. The assessment of each child was videotaped by a trained technician following a SOP for recording the assessment and editing for review by 2 to 3 other pediatric neurologists who were trained on implementing the scale. All were blinded to the subjects' treatment status. In the event of discrepancy of more than 1 point between the 2 blinded scorers, a 3rd pediatric neurologist, also blinded, scored the video in order to act as a tie-breaker. The final score was an average of the assessment of 3 to 4 reviewers (primary + 2 to 3 additional reviewers), minimizing bias and subjective interpretation. The data provided here is the final score.

² Subjects C1-C12, Cohort 2, participated in the control arm of the study.

³ Each subject typically underwent 2 to 3 motor and language assessments.

⁴ Motor score – Scale of 0-3, 3 is normal, 2 is abnormal, but independent, 1 is abnormal, requires assistance and 0 is Non-ambulatory

⁵ Language – Scale of 0-3, 3 is normal, 2 is abnormal, 1 is barely understandable, requires assistance and 0 is unintelligible or no speech

⁶ Composite of motor and language

Subject²	Study visit³	Age at assessment (months)	Time after first assessment (months)	Motor score⁴	Language score⁵	Total score⁶
C1	1	74.8	0	1.0	1.0	2.0
	2	85.8	+ 11.0	0.0	0.0	0.0
C2	1	55.3	0	1.3	2.0	3.0
	2	60.3	+ 5.0	1.3	1.0	2.3
	3	102.7	+ 47.4	0.0	0.0	0.0
C3	1	65.7	0	1.0	1.0	2.0
	2	70.8	+ 5.1	0.7	0.7	1.4
C4	1	47.8	0	1.0	1.0	2.0
	2	58.1	+ 10.4	0.0	0.3	0.3
C5	1	30.0	0	3.0	2.0	5.0
	2	50.7	+ 20.7	2.0	1.0	3.0
C6	1	51.5	0	1.0	2.0	3.0
	2	52.6	+ 1.1	1.0	2.0	3.0
	3	69.4	+ 18.0	0.0	0.0	0.0
C7	1	57.2	0	1.7	1.7	3.4
	2	60.2	+ 3.0	2.0	1.7	3.7
	3	74.6	+ 17.4	0.0	0.0	0.0
C8	1	62.2	0	3.0	2.0	5.0
	2	80.8	+ 18.6	1.0	1.0	2.0
C9	1	58.9	0	1.3	1.0	2.3
	2	65.5	+ 6.6	1.0	0.0	1.0
	3	81.7	+ 22.8	0.0	0.0	0.0
C10	1	56.4	0	1.0	1.3	2.3
	2	75.1	+ 18.6	0.0	0.0	0.0
C11	1	69.0	0	1.0	1.3	2.3
	2	85.1	+ 16.1	1.0	0.0	1.0
C12	1	59.7	0	1.0	1.3	2.3
	2	74.3	+ 14.6	1.0	0.7	1.7

Table S10. Inclusion/exclusion criteria for cohorts 1 and 2.¹

¹ All individuals who meet the following criteria will be included without bias as to a gender or race/ethnicity. Each case will be individually reviewed with the Eligibility Committee comprised of 3 physicians other than the PI, including a pediatric neurosurgeon, pediatric neurologist and general pediatrician.

² Natural history data from 140 genotype-confirmed CLN2 patients from two independent international cohorts (5), including our data, were analyzed to provide detailed longitudinal natural history data which demonstrated that the motor and language subscores of the clinical rating scales were an accurate predictor of disease progression and severity. The entire 12-point LINCL scale was used to determine inclusion/exclusion criteria for the study, while the motor + language data only were used to determine efficacy. This is similar to what was done to determine the efficacy of Brineura[®] (31).

Inclusion criteria

- Definitive diagnosis of CLN2 disease, based on clinical phenotype and genotype. The genotype must include at least one of the 5 of the following CLN2 mutant genotypes: C3670T (c.622 C>T, nonsense Arg208 to stop), G3556C (c.509-1G>C, intron 5, splice), G5271C (c.1266 G>C, Gln422His), and G4655A (c.1094G>A, Cys365Tyr). If either parental allele is R447H, the patient was not included in the study. These variants account for a total of 83% of the mutations in the 1999 study by Sleat et al (1), 52% in the recent variant compilation by Gardner et al (11), and 82% of the mutations in the population screened for the therapy vs no therapy study. Our data regarding the natural history of the disease and the studies of Steinfeld et al (63), demonstrate that, for these 5 genotypes (genetic constitution), CLN2 subjects have similar clinical course.
- The subject must be between the age of 2 and 18 years
- Subjects will have an average total score of 6 -12 on the Weill-Cornell LINCL scale and the total score should not be outside the 95th percentile confidence limits for age based on Worgall et al (4).
- The subject will not previously have participated in a gene therapy or stem cell study.
- Parents of study participants must agree to comply in good faith with the conditions of the study, including attending all of the required baseline and follow-up assessments, and both parents or legal guardians must give consent for their child's participation.
- Sexually active subjects will have to use contraception during the treatment and for 2 months after completion of the treatment.
- If asymptomatic but has one older sibling who has a positive genotype and has clinical manifestations of the disease.

Exclusion criteria:

- Presence of other significant medical or neurological conditions may disqualify the subject from participation in this study, particularly those which would create an unacceptable operative risk or risk to receiving the AAVrh.10hCLN2 vector, e.g., malignancy, congenital heart disease, liver or renal failure
 - Subjects without adequate control of seizures to screening, or active enrollment in an investigational medication or device study
 - Subjects with heart disease that would be a risk for anesthesia or a history of major risk factors for hemorrhage
 - Subjects who cannot participate in MRI studies
 - Concurrent participation in any other FDA approved Investigational New Drug
 - Subjects with history of prolonged bleeding or abnormal platelet function or taking aspirin
 - Renal disease or altered renal function as defined by serum creatinine >1.5 mg/dl at admission
 - Abnormal serum sodium, potassium calcium, magnesium, phosphate at grade III or IV by Division of AIDS Toxicity Scale
 - Hepatic disease or altered liver function as defined by SGPT >150 U/L, and or total bilirubin >1.3 mg/dL
 - Immunosuppression as defined by WBC < 3,000/ μ L at admission
 - Uncorrected coagulopathy during the baseline period defined as INR >1.4; PTT >35 sec; platelets <100,000/ mm^3
 - Anemia (hemoglobin < 11.0 g/dl at > 2 years of age, with normal serum iron studies)
-

Table S11. Timeline of the clinical study.^{1,31}

Footnotes for Supplemental Table III

■= test required □= test optional

- ¹ Parameters listed were mandatory for the study; additional parameters were assessed at the discretion of the physician caring for the individual based on general medical practice for similar neurosurgical procedure in this age group. Cohort 1 and 4 underwent all the tests at the time-points specified above and as specified for specific tests below. Cohort 2, the natural history control cohort (no therapy), underwent the assessments at the screening and the 18 month time-point only.
- ² Dose of AAVrh.10hCLN2 administered = 2.85×10^{11} - 9.0×10^{11} gc.
- ³ The “Screening” time was the initial eligibility screening assessment. This assessment was carried out under a “screening/control” protocol. Families of the eligible subjects were given the choice to enter the control group (No Therapy, cohort 2) or gene transfer group (Therapy, cohort 1). The subjects entering the gene transfer group were reassessed within 2 wk pre-transfer. This provides the required baseline safety parameters.
- ⁴ The “pre-transfer” studies were carried out within 2 wk of administration of the vector, with the exception of the CNS MRI study which had to be done within 24 hr of administration of the vector. If greater than 2 wk prior to administration of the vector, then all of the parameters were reevaluated (listed as “pre-transfer”).
- ⁵ The “general assessment” was used to make the diagnosis of LINCL on clinical grounds plus CLN2 genomic analysis; prior genomic analysis was accepted.
- ⁶ General – medical history, physical exam, vital signs (blood pressure, heart rate, respiratory rate, temperature).
- ⁷ Temperature – Parents/legal guardians measured the temperature of the subject every morning for the first three months post administration of the vector. If the temperature was above 38.5° C (101.3° F), the parents/legal guardians were required to report this to the Department of Genetic Medicine immediately.
- ⁸ CBC – complete blood count, included: hematocrit, hemoglobin, white blood count, differential, platelets.
- ⁹ ESR – erythrocyte sedimentation rate.
- ¹⁰ Clotting – prothrombin time, partial thromboplastin time.
- ¹¹ Chemistry – sodium, potassium, chloride, total CO₂, blood urea nitrogen (BUN), glucose, magnesium, uric acid, phosphate, creatinine, alanine amino transferase (SGPT), aspartate amino transferase (SGOT), calcium, serum total protein, albumin, alkaline phosphatase, bilirubin (total).
- ¹² Future (serum) – serum sample frozen for future use.
- ¹³ Blood type – necessary prior to the surgical procedure.
- ¹⁴ Urinalysis – appearance, specific gravity, pH, protein, glucose, ketones, bilirubin, number and type of cells, characterization of sediment.
- ¹⁵ Pregnancy test (urine): required for pubescent female.
- ¹⁶ EKG – electrocardiogram. If the subject had a cardiac history, previous EKG results were accepted if within 6 months of surgery or MRI provided it was read by a pediatric cardiologist. If no cardiac history was present, an EKG was not necessary.
- ¹⁷ Level of consciousness, speech, language, cranial nerves, motor strength, motor tone, abnormal movements, reflexes, upper extremity sensation, lower extremity sensations, gait, Romberg test, nystagmus, coordination.
- ¹⁸ Posterior-anterior. Subject’s previous chest x-ray was accepted if within 6 months of screening unless there was a significant change in his/her clinical scenario. The month 6 and 12 chest x-rays were optional and were only performed if there was a significant change in the subject’s clinical scenario since the previous x-ray.
- ¹⁹ For Cohorts 1 and 4 “Vector-related” studies included assessment of anti-AAVrh.10 neutralizing antibodies, anti-AAVrh.10 cellular response (ELISPOT), and anti-CLN2 cellular response (ELISPOT).
- ²⁰ For Cohorts 1 and 4 samples of CSF were collected under anesthesia. For safety purposes the CSF was assessed for CSF for routine parameters.
- ²¹ Routine ophthalmologic exam; this was carried out to help define the overall status of the LINCL. Anesthesia was administered depending on the ability of the subject to remain still as the doctor performs the tests. The eye exam may have included eye dilation, color photos, electroretinogram (ERG), fluorescein angiography and optical coherence tomography (OCT).
- ²² Subject’s family and/or physician were contacted monthly via telephone 1 month after receiving the vector.
- ²³ For cohorts 1 and 2, a clinical rating scale was administered that included assessment of motor + language parameters of the Weill-Cornell LINCL rating scale. This assessment was videotaped and reviewed by multiple neurologists as described in Methods.
- ²⁴ For Cohort 1, TPP1 levels were assessed in the CSF at one time-point pre and one time-point post administration.
- ²⁵ For Cohort 1 and 4, Magnetic Resonance Imaging (MRI) at 0 to 2 days was performed for assessment of safety and clinical post-operative care (exact time was determined at the discretion of the neurosurgeon); For cohorts 1 and 2, MRI studies were carried out to assess grey matter volume on the same scanner (3.0 Tesla).

Table S11. Timeline of the Clinical Study^{1,31} (cont., page 2)

- ²⁶ For Cohorts 1 and 2, the Child Health Questionnaire™ (CHQ) or Infant Toddler Quality of Life questionnaire (ITQoL) was administered to at least one parent/legal guardian at the designated visits. The ITQoL was developed for use infants and toddlers ages 2 months to 5 years old. The CHQ is a family of generic quality of life instruments that have been designed and normed for children 5-to-18 years of age.
- ²⁷ For Cohorts 1 and 2, the subjects were evaluated on the developmental scale and videotaped.
- ²⁸ The 2 month and 3 month evaluation procedures were performed by the subject’s local physician.
- ²⁹ It was possible to perform the 6, 12 and 18 month evaluation procedures locally at the request of the subject’s family. Though it was preferable for the subject and his/her family to return to NYPH-WCMC for the 6, 12 and 18 month follow-up visit, the study team coordinated with the subject’s family and/or physician to perform the parameters listed in the timeline of the protocol.
- ³⁰ For follow-up visits performed off-site: weight, future (serum), ophthalmology and lumbar puncture were optional at the 6, 12 or 18 month visit. CBC, clotting, chemistry and MRI were required at either the 6 or 12 month visit and optional at the 18 month visit. Test values from a recent clinical/ hospital visit was accepted if the study team was unable to obtain the measurements or samples during the off-site visit.
- ³¹ The acceptable “time windows” for the assessment days were as follows:

	Pre-vector	Day 7	Day 14	Month 1	Month 6	Month 12	Month 18	Year 2 to annual life time follow up
Screening parameters	8 months to 2 wks pre vector administration							
Pre-transfer (baseline) ^a	2 wk to -1 day prior to the vector administration							
Post vector		± 2 days	± 2 days	± 5 days	± 30 days	± 30 days	± 30 days	± 30 days

^a Except pre-transfer for the MRI/MRS which must be done within 24 hr of the vector administration

Table S12. Inclusion/exclusion criteria for cohort 4.¹

¹ All individuals who meet the following criteria will be included without bias as to a gender or race/ethnicity. Each case will be individually reviewed with the Eligibility Committee comprised of 3 physicians other than the PI, including a pediatric neurosurgeon, pediatric neurologist and general pediatrician.

Inclusion criteria

- Definitive diagnosis of CLN2 disease, based on clinical phenotype and genotype. If either parental allele is R447H, the patient was not included in the study. This genotype is associated with a late age at onset and protracted clinical phenotype (49, 50). No other genotype restriction.
- The subject must be between the age of 2 and 18 years.
- Subjects will have an average total score of <6 on the Weill-Cornell LINCL scale (4).
- The subject will not previously have participated in a gene transfer or stem cell study.
- Parents of study participants must agree to comply in good faith with the conditions of the study, including attending all of the required baseline and follow-up assessments, and both parents or legal guardians must give consent for their child's participation.
- Sexually active subjects will have to use contraception during the treatment and for 2 months after completion of the treatment.
- Parents accept inclusion in the treated safety only group (cohort 4).

Exclusion criteria

- Presence of other significant medical or neurological conditions may disqualify the subject from participation in this study, particularly those which would create an unacceptable operative risk or risk to receiving the AAVrh.10hCLN2 vector, e.g., malignancy, congenital heart disease, liver or renal failure.
 - Subjects without adequate control of seizures to screening, or active enrollment in an investigational medication or device study.
 - Subjects with heart disease that would be a risk for anesthesia or a history of major risk factors for hemorrhage.
 - Subjects who cannot participate in MRI studies.
 - Concurrent participation in any other FDA approved Investigational New Drug.
 - Subjects with history of prolonged bleeding or abnormal platelet function or taking aspirin.
 - Renal disease or altered renal function as defined by serum creatinine >1.5 mg/dl at admission.
 - Abnormal serum sodium, potassium calcium, magnesium, phosphate at grade III or IV by Division of AIDS Toxicity Scale.
 - Hepatic disease or altered liver function as defined by SGPT >150 U/L, and or total bilirubin >1.3 mg/dL.
 - Immunosuppression as defined by WBC <3,000/ μ L at admission.
 - Uncorrected coagulopathy during the baseline period defined as INR >1.4; PTT >35 sec; PLT < 100,000/ mm^3 .
 - Anemia (hemoglobin <11.0 g/dl at >2 years of age, with normal serum iron studies).
-